frontiers | Frontiers in Plant Science

REVIEW
published: 07 July 2022
doi: 10.3389/fpls.2022.929532

Mimicking the Oxygen-Evolving Center in Photosynthesis

Yang Chen[1,2†], Boran Xu[1,2†], Ruoqing Yao[1,2], Changhui Chen[1] and Chunxi Zhang[1*]*

[1]*Laboratory of Photochemistry, Institute of Chemistry, Chinese Academy of Sciences, Beijing, China,* [2]*University of Chinese Academy of Sciences, Beijing, China*

The oxygen-evolving center (OEC) in photosystem II (PSII) of oxygenic photosynthetic organisms is a unique heterometallic-oxide Mn_4CaO_5-cluster that catalyzes water splitting into electrons, protons, and molecular oxygen through a five-state cycle (S_n, $n = 0 \sim 4$). It serves as the blueprint for the developing of the man-made water-splitting catalysts to generate solar fuel in artificial photosynthesis. Understanding the structure–function relationship of this natural catalyst is a great challenge and a long-standing issue, which is severely restricted by the lack of a precise chemical model for this heterometallic-oxide cluster. However, it is a great challenge for chemists to precisely mimic the OEC in a laboratory. Recently, significant advances have been achieved and a series of artificial Mn_4XO_4-clusters (X = Ca/Y/Gd) have been reported, which closely mimic both the geometric structure and the electronic structure, as well as the redox property of the OEC. These new advances provide a structurally well-defined molecular platform to study the structure–function relationship of the OEC and shed new light on the design of efficient catalysts for the water-splitting reaction in artificial photosynthesis.

Keywords: photosystem II, oxygen-evolving center, Mn_4CaO_4-cluster, artificial photosynthesis, water-splitting reaction

OPEN ACCESS

Edited by:
Harvey J. M. Hou, Alabama State University, United States

Reviewed by:
Mohammad Mahdi Najafpour, Institute for Advanced Studies in Basic Sciences (IASBS), Iran
Govindjee Govindjee, University of Illinois at Urbana-Champaign, United States
Yulia Pushkar, Purdue University, United States

***Correspondence:**
Changhui Chen
chenchanghui@iccas.ac.cn
Chunxi Zhang
chunxizhang@iccas.ac.cn

†These authors have contributed equally to this work

Specialty section:
This article was submitted to Plant Physiology, a section of the journal Frontiers in Plant Science

Received: *27 April 2022*
Accepted: *20 June 2022*
Published: *07 July 2022*

Citation:
Chen Y, Xu B, Yao R, Chen C and Zhang C (2022) Mimicking the Oxygen-Evolving Center in Photosynthesis. Front. Plant Sci. 13:929532. doi: 10.3389/fpls.2022.929532

INTRODUCTION

Photosynthetic oxygen evolution is a unique function of oxygenic photosynthetic organisms, which takes place in photosystem II (PSII) of cyanobacteria, algae, and plants (Barber, 2009; Dau and Zaharieva, 2009; Cardona et al., 2012; Vinyard et al., 2013; Shen, 2015; Govindjee et al., 2017; Junge, 2019; Lubitz et al., 2019; Shevela et al., 2019; Blankenship, 2021). PSII is a multi-subunit membrane protein complex containing more than 20 subunits and hundreds of cofactors. The reaction center of PSII is shown in **Figure 1A**. Upon photo excitation, the primary electron donor (P_{680}) donates one electron to the primary electron acceptor (Pheo) in a few picoseconds, producing the $P_{680}^{+\bullet}$ and $Pheo^{-\bullet}$ at the donor side and acceptor side, respectively (Renger and Holzwarth, 2005; Rappaport and Diner, 2008; Cardona et al., 2012; Shevela et al., 2021). $Pheo^{-\bullet}$ then delivers the electron to the primary plastoquinone (Q_A) and the secondary plastoquinone (Q_B) in sequence *via* the non-heme iron at the acceptor side (Petrouleas and Crofts, 2005; Cardona et al., 2012), where one bicarbonate anion coordinated on the non-heme iron is highly required for the efficient electron transfer between Q_A and Q_B (Shevela et al., 2012). $P_{680}^{+\bullet}$ with high redox potential (~1.25 V) abstracts one electron from the secondary electron donor (Tyr_Z), forming a neutral radical ($Tyr_Z^{\bullet}$) (Diner and Britt, 2005; Styring et al., 2012). The latter then drives the water-splitting reaction at the oxygen-evolving center (OEC) in

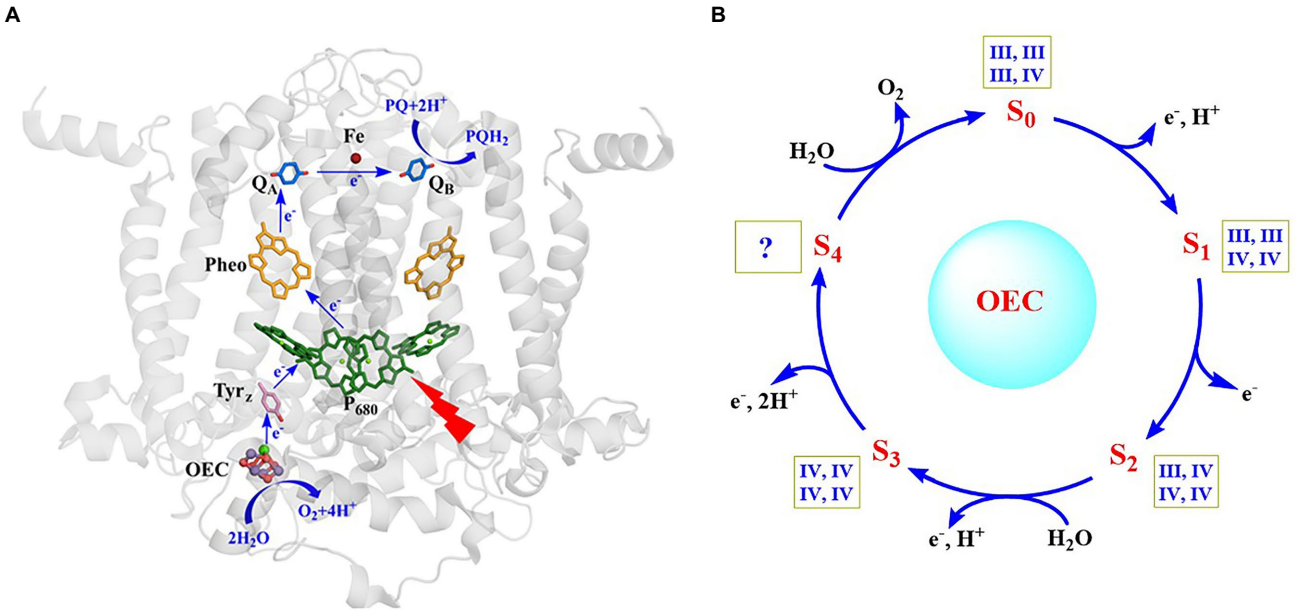

FIGURE 1 | Structure of the reaction center and main cofactors involved in electron transfer in PSII (Umena et al., 2011) **(A)** and catalytic cycle of the OEC (Cox et al., 2020) **(B)**. The oxidation states of four Mn ions in each S-state are shown within square boxes.

milliseconds at the donor side (Tommos and Babcock, 1998; Zhang, 2007; Styring et al., 2012). The catalytic turnover of the OEC (**Figure 1B**) involves five different redox states (S_n, $n=0\sim4$) (Kok et al., 1970; Dau and Haumann, 2007; Cox et al., 2014a; Yano and Yachandra, 2014), in which the S_0 state is the initial and most reduced state, the S_1 state is the dark-stable state, the S_2 and S_3 states are metastable and decay eventually to the dark stable S_1 state, whereas the S_4 state is a transient state that releases molecular oxygen and regenerates the S_0 state. This catalytic water-splitting reaction provides electrons and protons to, ultimately, produce the biomass or biofuel, and molecular oxygen to maintain the oxygenic atmosphere of our planet (Blankenship et al., 2011; Barber, 2020), which serves as the blueprint to develop efficient man-made catalysts for the water-splitting reaction in artificial photosynthesis.

Due to broad interests in fundamental research and potential applications in artificial photosynthesis (Herrero et al., 2008; Gust et al., 2010; Andreiadis et al., 2011; Concepcion et al., 2012; Faunce et al., 2013; Kärkäs et al., 2014; Hunter et al., 2016; Najafpour et al., 2016; El-Khouly et al., 2017; Nocera, 2017; Ye et al., 2019; Zhang and Sun, 2019b; Zhang and Reisner, 2020; Kondo et al., 2021), the structure and catalytic mechanism of the OEC have attracted extensive attention during the last century (Junge, 2019; Cox et al., 2020). However, revealing the principle of the OEC has been one of the great and persistent challenges and a long-standing issue in the research field of photosynthesis.

STRUCTURE OF THE OEC

Extensive biochemistry and biophysics studies have been performed to reveal the properties of the OEC in different S-states during the last several decades (Yano and Yachandra, 2014; Junge, 2019). It has been well demonstrated that OEC is composed of four Mn ions and one calcium ion, in which the calcium can be replaced by strontium (Debus, 1992; Yocum, 2008). Based on spectroscopic studies of the X-ray absorption spectroscopy (XAS) (Yano and Yachandra, 2014) and electron paramagnetic resonance (EPR) (Peloquin and Britt, 2001; Krewald et al., 2015) measurements of different S-states OEC, the oxidation states of the four Mn ions were generally suggested to be S_0 (III, III, III, IV), S_1 (III, III, IV, IV), S_2 (III, IV, IV, IV), and S_3 (IV, IV, IV, IV), respectively. However, some groups (Zheng and Dismukes, 1996; Gatt et al., 2012; Pace et al., 2012; Petrie et al., 2020) suggested that the oxidation states of the four Mn ions could be S_0 (II, III, III, III), S_1 (III, III, III, III), S_2 (III, III, III, IV), and S_3 (III, III, IV, IV), respectively. These two different assignments of the four Mn ions are labeled as the "high-oxidation paradigm" and the "low oxidation paradigm," respectively (Krewald et al., 2015; Pantazis, 2018). The former has generally been used by most researchers, yet the unambiguous chemical evidence for the assignment of the oxidation states of the four Mn ions remains elusive.

The crystal structure information of the OEC has emerged since the beginning of this century (Zouni et al., 2001; Kamiya and Shen, 2003; Ferreira et al., 2004; Loll et al., 2005; Guskov et al., 2009; Tanaka et al., 2017; Graça et al., 2021; Kato et al., 2021). In 2001, Zouni et al. reported a crystal structure of PSII from a cyanobacterium at a resolution of 3.8 Å (Zouni et al., 2001). In 2004, Ferreira et al. (Ferreira et al., 2004) reported a resolution of 3.5 Å structure data of PSII and proposed that the OEC was a Mn_3CaO_4 cubane attached by a "dangler" Mn ion *via* one μ_4-oxide bridge, forming a Mn_4CaO_4-cluster (Ferreira et al., 2004). In 2011, Umena et al. (Umena et al., 2011) reported the crystal structure of PSII at a resolution of 1.9 Å, which revealed

the detailed structure of the OEC, as shown in **Figure 2A**. Here, the coordination ligands of the OEC are provided by six carboxylate groups from the amino acid residues of D_1-Asp_{170}, D_1-Glu_{189}, D_1-Glu_{333}, D_1-Asp_{342}, D_1-Ala_{344}, CP_{43}-Glu_{354}, one imidazole group from D_1-His_{332}, and four water molecules (two on calcium and two on dangler Mn, respectively). Further, an additional μ_2-oxide bridge (O4) between Mn4 and Mn3 was observed (Umena et al., 2011), which is consistent with the proposal by Dau et al. (2008). The structure of the OEC, shown in **Figure 2A**, has been further confirmed by the X-ray free-electron laser (XFEL) data (Kupitz et al., 2014; Suga et al., 2015, 2017, 2019; Young et al., 2016; Kern et al., 2018; Ibrahim et al., 2020; Hussein et al., 2021) and the single-particle cryo-electron microscopy (Cryo-EM) (Wei et al., 2016; Kato et al., 2021; Xiao et al., 2021; Gisriel et al., 2022). The entire structure of the OEC is an asymmetric Mn_4CaO_5-cluster. In this cluster, calcium, a key component of the OEC, is located in the middle and connected to the four Mn ions through three oxide bridges and two carboxylate groups; this structural feature (see **Figure 2B**) is consistent with the proposal by Zhang et al. in 1999 (Zhang et al., 1999).

Notably, most crystallographic studies, in the past, were performed on the dark stable PSII sample, in which the OEC was generally in the S_1 state. Recently, the structures of the OEC in other S-states have been reported (Suga et al., 2017, 2019; Kern et al., 2018; Ibrahim et al., 2020; Hussein et al., 2021; Li et al., 2021). Remarkably, one new oxygen atom (O_6) coordinated to the Mn1 was observed in the S_3 state. This new oxygen atom was suggested to serve as one of the substrates to form the O=O bond (Suga et al., 2017, 2019; Kern et al., 2018; Ibrahim et al., 2020). However, the existence of the new oxygen (O_6) in the S_3 state is still under debate. It was argued that both O_6 and O_5 in the reported S_3 state OEC may belong to the same oxygen atom but in two possible positions (Petrie et al., 2020; Wang et al., 2021). Furthermore, there are some structural uncertainties due to the incoherent transition of the S-state of PSII samples (Askerka et al., 2015; Tanaka et al., 2017).

Compared with the structure revealed by the X-ray diffraction (XRD) (Ferreira et al., 2004; Loll et al., 2005; Umena et al., 2011; Tanaka et al., 2017), the structure of the OEC revealed by the XFEL (Kupitz et al., 2014; Suga et al., 2015, 2017, 2019; Young et al., 2016; Kern et al., 2018; Ibrahim et al., 2020; Hussein et al., 2021) has been considered to be more reliable due to the lack of significant radiation damage induced by the X-ray beam (Yano et al., 2005; Grabolle et al., 2006). However, as yet, there is consensus for the atomic positions of the S_1 state OEC, as revealed by XFEL, certainly not for all structures with the results from EXAFS spectroscopy studies on the active sample used (Davis and Pushkar, 2015; Askerka et al., 2017). To check if those reported structure data were directly correlated with the native structures of the OEC in different S-states, we have carried out bond valence sum (BVS) calculations on these XFEL's structures reported recently (Chen et al., 2019; Li et al., 2020b). We note that BVS calculation has been widely used to evaluate the oxidation valences of atoms in coordination complexes and in metalloenzymes (Brown, 2009). **Table 1** lists the results of the BVS calculation on the XFEL's structures of different S-states of the OEC reported recently. Surprisingly, we see that the oxidation states of the four Mn ions revealed by BVS calculations are significantly lower than that suggested by the spectroscopic studies (Peloquin and Britt, 2001; Dau and Haumann, 2007; Yano and Yachandra, 2014; Krewald et al., 2015) (**Figure 1B**), indicating that the reduction of the Mn ions with high valences would take place during the structural determination by XFEL (Yano et al., 2005; Grabolle et al., 2006; Amin et al., 2016). If so, one would expect that those reported structure data of the OEC would be different from the native structure. This opinion is consistent with the suggestion that structural modifications of the OEC induced by XFEL may take place and the position of the

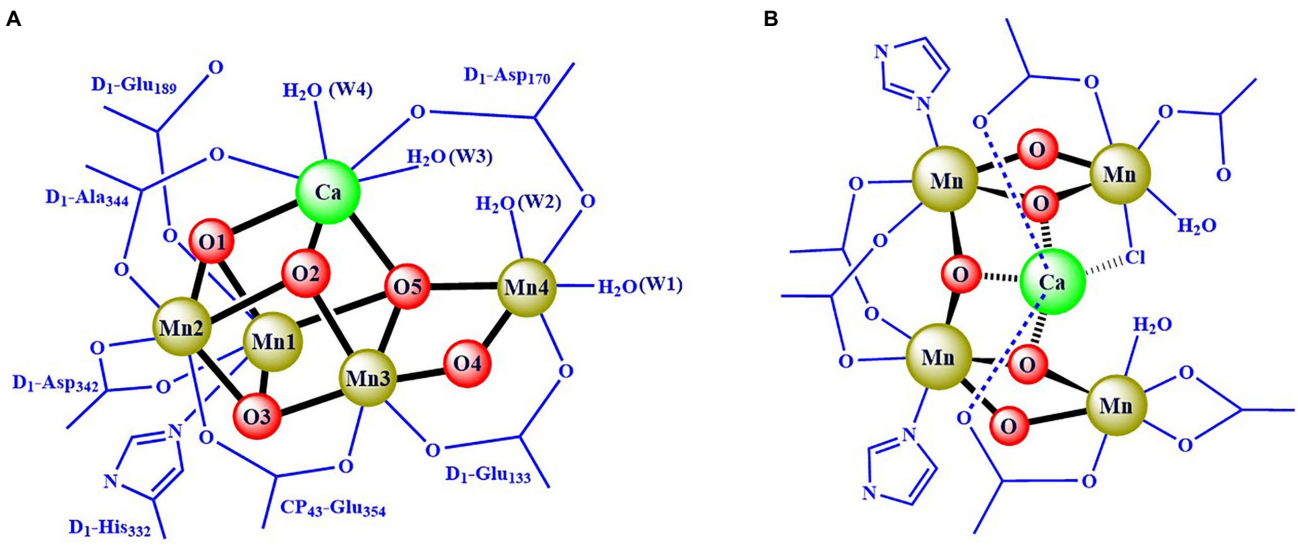

FIGURE 2 | Scheme for the structure of the OEC (Umena et al., 2011) **(A)** and the theoretical model (Zhang et al. 1999) **(B)**.

TABLE 1 | Bond valence sum (BVS) calculations on the structure of the OEC revealed by X-ray free-electron laser (XFEL) method at different resolutions in different S-states.

	S_1 (1.95 Å) 4UB6	S_1 (2.05 Å) 6DHE	S_2 (2.15 Å) 6JLK	S_2 (2.08 Å) 6DHF	S_3 (2.07 Å) 6DHO	S_3 (2.15 Å) 6JLL
Mn1	3.075 (III)	3.101(III)	3.000(III)	3.232(III)	3.901(IV)	4.203(IV)
Mn2	3.237 (III)	4.277(IV)	3.735(IV)	4.316(IV)	4.193(IV)	3.792(IV)
Mn3	2.980 (III)	3.670(IV)	2.946(III)	3.784(IV)	3.232(III)	3.181(III)
Mn4	2.318 (II)	2.870(III)	2.623(III)	3.139(III)	2.932(III)	2.551(II)

Roman numerals in parentheses indicate the assignment of the oxidation state of Mn ion based on BVS calculation. All atomic coordinates used for BVS calculation were taken from the first monomer of PS II in the crystal structure data with PDB-IDs: 4UB6 (Suga et al., 2015), 6DHE (Kern et al., 2018), 6DHF (Kern et al., 2018), 6DHO (Kern et al., 2018), 6JLK (Suga et al., 2019), and 6JLL (Suga et al., 2019), respectively.

oxide bridge (eg., O_5) could be significantly disturbed by XFEL (Amin et al., 2016). Therefore, the precise structure of the OEC in different S-states remains elusive.

CATALYTIC MECHANISM OF THE OEC

Based on biochemical, biophysical, and theoretical investigations, various hypotheses for the catalytic mechanisms of the O=O bond formation have been suggested by many researchers (Siegbahn, 2013; Askerka et al., 2017; Barber, 2017; Wang et al., 2017; Corry and O'Malley, 2018; Kawashima et al., 2018; Kern et al., 2018; Pushkar et al., 2018; Yamaguchi et al., 2018; Britt and Marchiori, 2019; Suga et al., 2019; Zhang and Sun, 2019a; Marchiori et al., 2020; Capone et al., 2021). **Figure 3** shows four typical proposals.

Figure 3A shows a possible mechanism proposed by Barber (Barber, 2017), in which two water molecules (W2 and W3) serve as substrates to form the O=O bond. The key feature of this mechanism is that the O=O bond is formed by a nucleophilic attack of a calcium ligated hydroxyl group onto an electrophilic oxo group of $Mn^{V}\equiv O$ or Mn^{IV}-O• derived from the deprotonation of the second substrate water molecule. Similar proposals had also been suggested by others (Pecoraro et al., 1998; Vrettos et al., 2001; Chen et al., 2015; Vinyard et al., 2015). However, these proposals were not supported by recent theoretical calculations reported by Siegbahn group (Siegbahn, 2017). The second model (**Figure 3B**) was suggested by Ishikita group (Kawashima et al., 2018), in which the μ_2-oxide bridge (O4) and one water molecule (W1) serve as two oxygen sources to form the O=O bond. The key feature of this proposal is that the O=O bond is formed through the coupling of the O4 oxide bridge and a Mn^{IV}-O• oxyl radical. However, the oxidation states of (III, IV, IV, IV) for the four Mn ions in the S_3 state were not consistent with the widely accepted oxidation states of (IV, IV, IV, IV) (Peloquin and Britt, 2001; Dau and Haumann, 2008; Yano and Yachandra, 2014; Krewald et al., 2015). The third model (**Figure 3C**) was proposed by Sun group (Zhang and Sun, 2019a), in which one Mn^{VII} ion was suggested to be involved in the S_4 state. This mechanism has been recently evaluated by a computational study that shows that the formation of the Mn^{VII} requires a much higher barrier for forming O_2 than the earlier proposals with four Mn^{IV} atoms (Li et al., 2020a). The fourth model, originally proposed by Siegbahn (Siegbahn, 2013), and then other groups (Pecoraro et al., 1998; Cox et al., 2020), is where the μ_4-oxide bridge (O5) and the newly inserted water (O_6) are considered to serve as the oxygen source for the O=O bond (**Figure 3D**). This proposal has been widely used to explain the observation of the crystallographic data and a large number of spectroscopic observations (Cox et al., 2014b, 2020; Kern et al., 2018; Britt and Marchiori, 2019; Suga et al., 2019). According to this mechanism, the release of O_2 from the S_4 state would result in the formation of four unsaturated metal ions, namely three 5-coordinated manganese (i.e., Mn1, Mn3, and Mn4) and one 6-coordinated calcium, which would certainly require a much higher activation energy (Zhang and Kuang, 2018). Thus, one would expect that the molecular oxygen release could be the rate-limiting step during the catalytic cycle; however, this is inconsistent with the fast O_2 release observed in PSII (Haumann et al., 2005; Davis et al., 2018).

As mentioned above, although various hypotheses for the mechanism of the water-splitting reaction of the OEC have been proposed (Siegbahn, 2013; Askerka et al., 2017; Barber, 2017; Wang et al., 2017; Corry and O'Malley, 2018; Kawashima et al., 2018; Kern et al., 2018; Pushkar et al., 2018; Yamaguchi et al., 2018; Britt and Marchiori, 2019; Suga et al., 2019; Zhang and Sun, 2019a; Marchiori et al., 2020; Capone et al., 2021), the detailed mechanism remains an open question mainly due to the lack of the unambiguous experimental evidence for the O=O bond formation and the precise geometric structure and electronic structure of the OEC in different S-states (Chen and Zhang, 2021).

MIMICKING THE OEC

To facilitate the understanding of the structure and properties of the OEC, as well as for developing efficient water-splitting catalysts, many research groups, during the last three decades, have attempted to synthesize the OEC (Wieghardt, 1989; Limburg et al., 1999; Mukhopadhyay et al., 2004; Mullins and Pecoraro, 2008; Dismukes et al., 2009; Gerey et al., 2016; Zhang and Sun, 2019b; Li et al., 2020b; Chen et al., 2021; Ezhov et al., 2021). It is a great challenge and a long-standing issue for chemists to synthesize the OEC in the laboratory (Zhang, 2015; Li et al., 2020b). During the last two decades, numerous multi-manganese complexes have been synthesized (Wieghardt, 1989; Limburg et al., 1999; Mukhopadhyay et al., 2004; Mullins and Pecoraro, 2008; Dismukes et al., 2009; Gerey

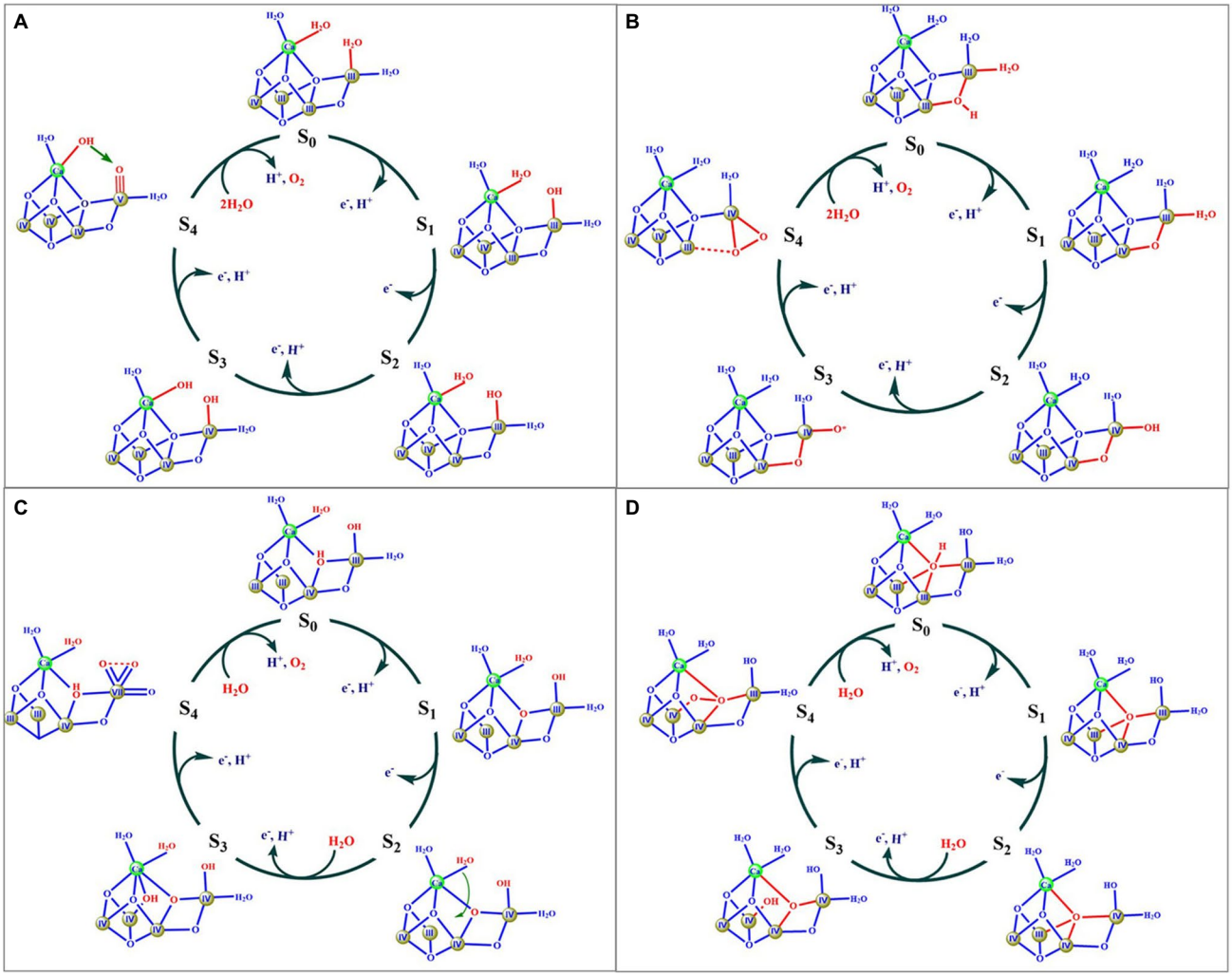

FIGURE 3 | Four typical mechanism models suggested in literatures. Components of the OEC involved in O=O bond formation are marked by red color. Roman numbers indicate the oxidation state of the Mn ion.

et al., 2016; Chang et al., 2017). Significant advances for the mimicking of the OEC have emerged since 2011 (Tsui et al., 2013a; Chen et al., 2017; Paul et al., 2017). Further, Agapie group (Kanady et al., 2011) reported an artificial $Mn^{IV}_3CaO_4$-complex (**1**) using a multi-pyridylalkoxide ligand (**Figures 4A,B**). In addition, a series of analogs or derivatives of the cluster have been reported, by using a similar ligand (Tsui and Agapie, 2013; Kanady et al., 2014; Lin et al., 2015; Lionetti et al., 2019). In 2012, Christou group reported a $Mn^{IV}_3Ca_2O_4$-complex (**2**) with one Ca^{2+} attached to the Mn_3CaO_4 cubane (Mukherjee et al., 2012) (**Figures 4C,D**). A similar $Mn_3Ca_2O_4$-complex was also isolated as a by-product during the synthesis of Mn_4CaO_4-cluster (Chen et al., 2022). Here, the peripheral ligands of the $Mn_3Ca_2O_4$-cluster are provided by pivalic anions or neutral pivalic acid, which resembles to that of the OEC in PSII (Umena et al., 2011). In 2014, Zhang group (Chen et al., 2014) reported an artificial $(Mn^{IV}_3SrO_4)_2O$-complex (**3**) that contains both the heterometallic-oxide Mn_3SrO_4 cubane and all three types of oxide bridges (μ_2-oxide, μ_3-oxide, and μ_4-oxide), as seen in the Sr^{2+}-containing OEC (Koua et al., 2013) (**Figures 4E,F**).

In 2015, Zhang group reported an artificial Mn_4CaO_4-complex (**4**; **Figures 5C,D**) that was prepared through a two-step procedure (Zhang et al., 2015). The first step was to synthesize a precursor through a reaction of $Ca(CH_3CO_2)_2{\bullet}H_2O$, $Mn(CH_3CO_2)_2{\bullet}(H_2O)_4$, $^nBu_4NMnO_4$ (^{n}Bu = n-butyl), and ^{t}BuCO$_2$H (^{t}Bu = tert-butyl; molar ratio of 1: 1: 4: 40) in boiling acetonitrile. The second step was to treat the precursor with 2% pyridine in ethyl acetate, leading to the formation of the final product, $[Mn_4CaO_4(^tBuCO_2)_8(^tBuCO_2H)_2(C_5H_5N)]$ (**4**). This Mn_4CaO_4-complex contains a Mn_3CaO_4 cubane attached by a dangler Mn ion *via* one μ_4-oxide bridge, forming an asymmetric Mn_4CaO_4-cluster. Its peripheral environment is provided by eight ^{t}BuCO$_2^-$ anions and three neutral ligands on Ca and Mn4 (two pivalic acid molecules and one pyridine, respectively),

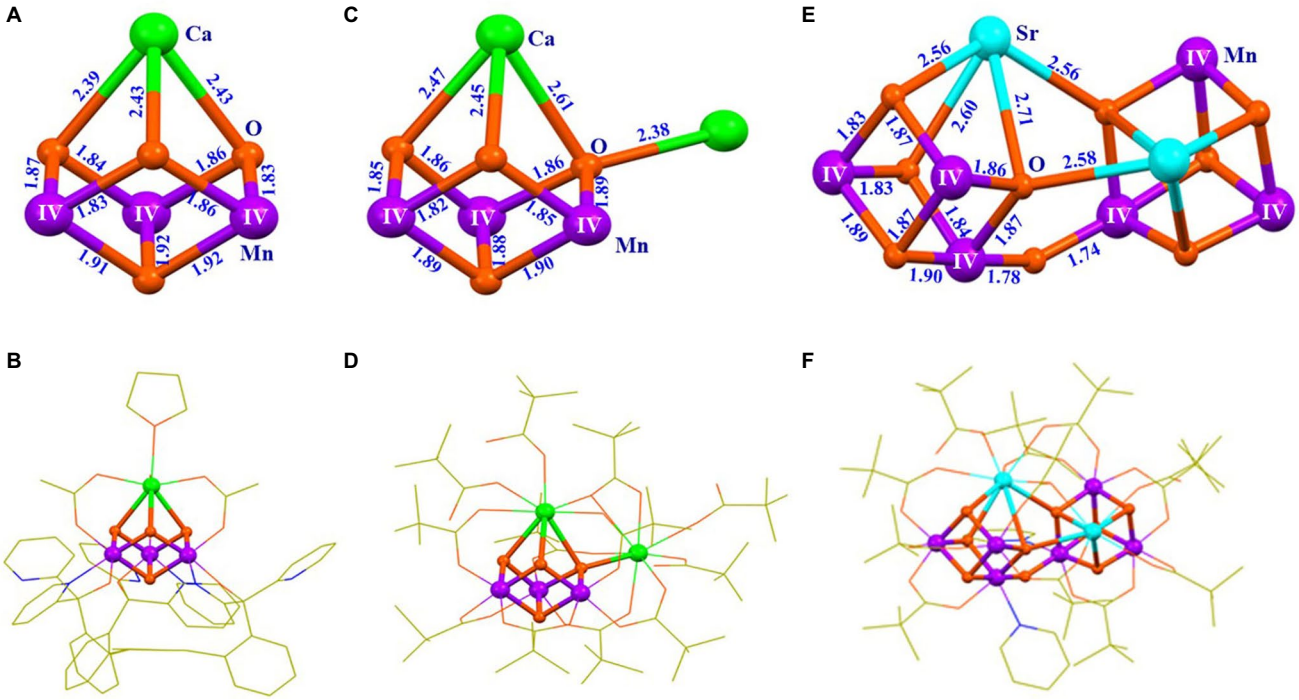

FIGURE 4 | Structures of three artificial complexes containing Mn_3XO_4 cubane (X = Ca/Sr). **(A)** Core of the Mn_3CaO_4-complex (**1**); **(B)** Structure of the Mn_3CaO_4-complex (**1**) (Kanady et al., 2011); **(C)** Core structure of the $Mn_3Ca_2O_4$-complex (**2**); **(D)** Structure of the $Mn_3Ca_2O_4$-complex (**2**) (Mukherjee et al., 2012); **(E)** Core of the $(Mn_3SrO_4)_2O$-complex (**3**); **(F)** Structure of the $(Mn_3SrO_4)_2O$-complex (**3**) (Chen et al., 2014). Distances are given in Å units; Mn, Ca, Sr., O, N, and C are shown in purple, green, cyan, orange, blue, and yellow, respectively. For clarity, all hydrogen atoms are not shown.

which is remarkably similar to that in the OEC. BVS calculation confirms that the oxidation states of the four Mn ions are in (III, III, IV, IV).

The artificial Mn_4CaO_4-cluster (**4**) has a $[Mn^{III}{}_2Mn^{IV}{}_2]$/$[Mn^{III}Mn^{IV}{}_3]$ redox couple of ~0.8 V (vs. normal hydrogen electrode, NHE), as shown in the cyclic voltammogram (CV) (**Figure 6A**), which is essentially the same as the estimated value (~ 0.8 V) for the $S_1 \rightarrow S_2$ transition of the OEC (Vass and Styring, 1991; Dau and Zaharieva, 2009; Mandal et al., 2020). The oxidized Mn_4CaO_4-cluster displays two distinct electron paramagnetic resonance (EPR) signals ($g = 4.9$ and $g = 2.0$) (**Figure 6B**), which are similar to the $g \approx 4$ and $g = 2.0$ EPR signals observed in the S_2 state OEC (Peloquin and Britt, 2001; Pantazis et al., 2012). Furthermore, the artificial Mn_4CaO_4-cluster can catalyze the water-splitting reaction on the electron surface in the presence of a small amount of water in acetonitrile (**Figure 6C**).

The artificial Mn_4CaO_4-cluster (**4**) is the closest mimic of the OEC up to now, which resembles not only in the structure of the metal-oxide core and the peripheral ligands, but also in the redox potential and the catalytic function of the OEC. Considering the high similarity between the artificial Mn_4CaO_4-cluster and the OEC, we speculate that oxidation states (III, III, IV, IV) of the four Mn ions in this artificial cluster provide unambiguous chemical evidence to support the assignment of oxidation states of (III, III, IV, IV) for the four Mn ions in the S_1 state OEC in PSII.

SYNTHESIZING MECHANISM OF THE MN_4CAO_4-CLUSTER

The mechanism of the synthesis of the artificial Mn_4CaO_4-cluster has been recently studied by characterizing the intermediate species during the synthesis of the Mn_4CaO_4-complex (**4**) (Chen et al., 2022). By using the high-resolution electrospray ionization (HR-ESI) mass spectroscopy, we have characterized the precursor of the Mn_4CaO_4-cluster and observed five key fragments with m/z^- values at 1233. 235, 1218.259, 875.118, 358.120, and 343.143 assigned to the $[Mn_4CaO_4(^tBuCO_2)_9]^-$, $[Mn_3Ca_2O_4(^tBuCO_2)_9]^-$, $[Mn_3CaO_4(^tBuCO_2)_6]^-$, $[Mn(^tBuCO_2)_3]^-$, and $[Ca(^tBuCO_2)_3]^-$, respectively (Chen et al., 2022). More importantly, after extensive experimentation, three key intermediates, $[Mn_3CaO_4(^tBuCO_2)_6(^tBuCO_2H)_3]$ (**5**), $[^nBu_4NMn(^tBuCO_2)_4]$ (**6**), and $[Mn_4CaO_4(^tBuCO_2)_8(^tBuCO_2H)_3]$ (**7**), were successfully crystallized. The structures of these intermediates (**5**–**7**) are shown in **Figure 7**.

Based on the isolation and characterization of these intermediates for the synthesis of the Mn_4CaO_4-cluster, we suggest that the Mn_4CaO_4-cluster could be formed through a reaction between a thermodynamically stable Mn_3CaO_4-cluster and an unusual four-coordinated Mn^{III} ion (**Figure 8**). The freshly formed Mn_4CaO_4-cluster (**7**) with carboxylate groups only is unstable, but it can be significantly stabilized by binding an organic base (e.g., pyridine) on the "dangler" Mn ion. Furthermore, we have found that the dangler Mn ion is flexible and can be replaced by calcium under weak

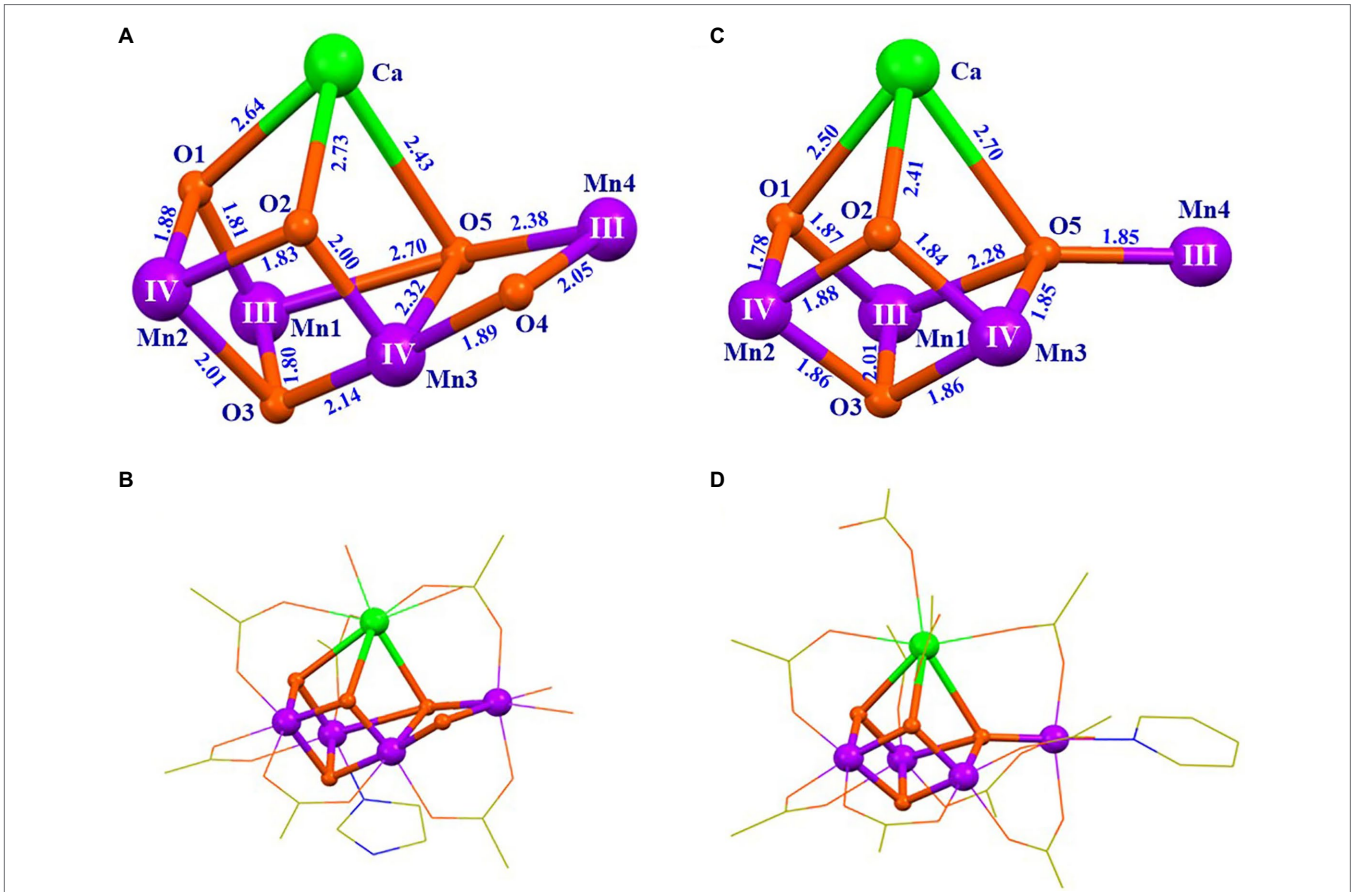

FIGURE 5 | Structural comparison of the OEC (Suga et al., 2015) and the artificial Mn_4CaO_4-complex (**4**) (Zhang et al., 2015). **(A)** Core of the OEC; **(B)** structure of the OEC; **(C)** core of **4**; **(D)** structure of **4**. The data for the OEC is taken from the first monomer in the crystal structure data of PSII with the Protein Data Bank code 4UB6. For clarity, the methyl groups and the hydrogen atoms are not shown. All other illustrations are the same as those in **Figure 4**.

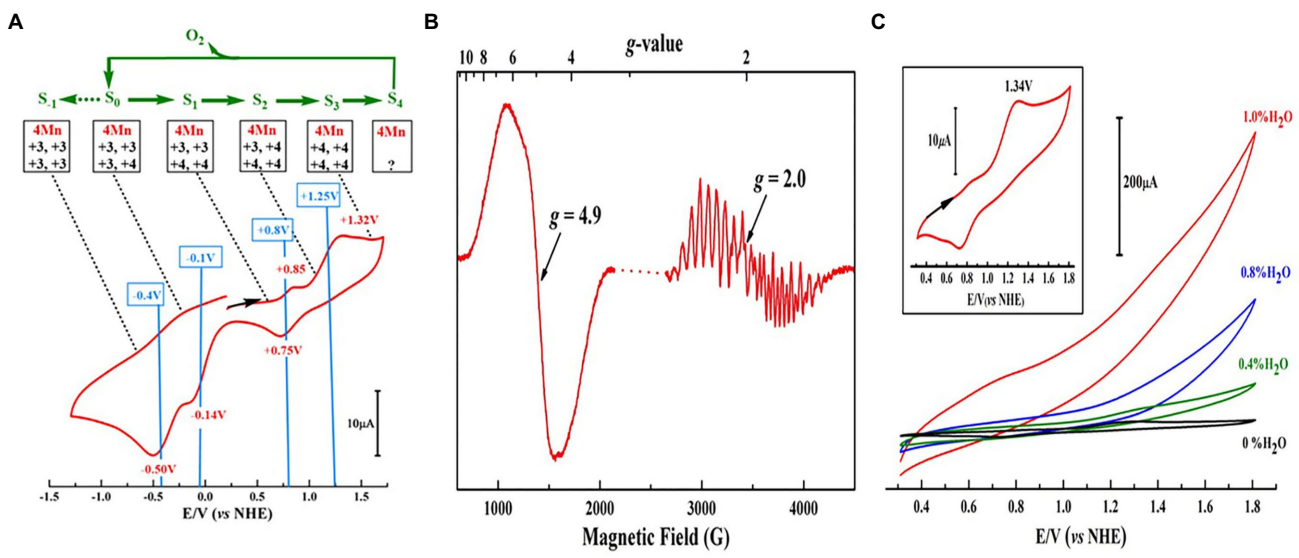

FIGURE 6 | Redox properties, EPR, and catalytic activity measurements of Mn_4CaO_4-complex (**4**) (Zhang et al., 2015). **(A)** Cyclic voltammogram (CV) measurement of **4** in dichloroethane; **(B)** EPR spectrum for the one-electron oxidized **4**; **(C)** activity measurements of **4** in acetonitrile with different amounts of H_2O. The inset in **C** shows the CV of **4** without H_2O on a different scale.

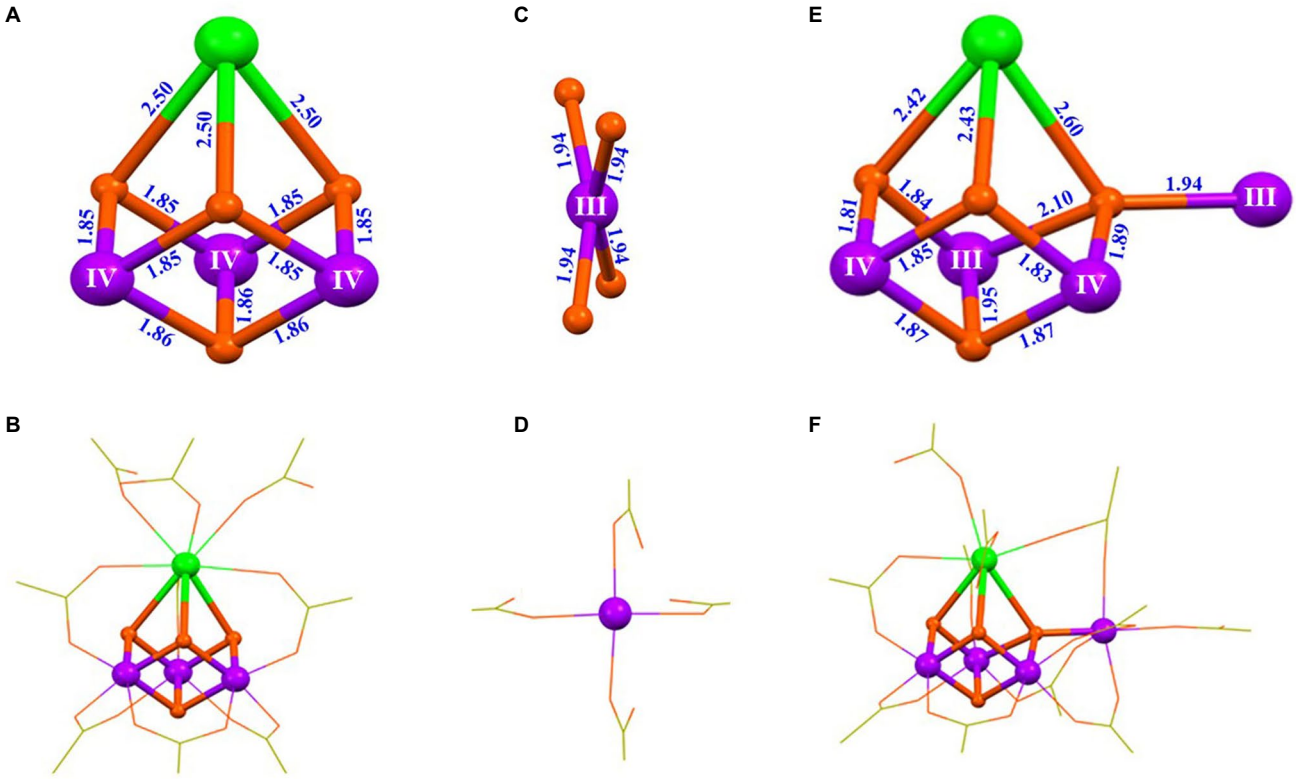

FIGURE 7 | Structures of three intermediates for the synthesis of the artificial Mn_4CaO_4-cluster (Chen et al., 2022). **(A)** Core of $[Mn_3CaO_4(tBuCO_2)_6(tBuCO_2H)_3]$ (**5**); **(B)** structure of **5**; **(C)** Mn center in $[^nBu_4NMn(^tBuCO_2)_4]$ (**6**); **(D)** structure of the $[Mn(^tBuCO_2)_4]^-$ anion in **6**; **(E)** core structure of $[Mn_4CaO_4(^tBuCO_2)_8(^tBuCO_2H)_3]$ (**7**); **(F)** structure of **7**. All other illustrations are the same as those in **Figure 5**.

acid conditions, giving rise to the $Mn_3Ca_2O_4$-cluster (**2**) as shown in **Figures 4C,D**.

Considering the high similarity between the artificial Mn_4CaO_4-cluster and the OEC (**Figure 5**), we speculate that the synthesizing mechanism (**Figure 8**), described above, could provide chemical insights into the assembly of the OEC. In the biological system, both the assembly and the disassembly of the OEC frequently take place under physiological conditions. The disassembly of the OEC takes place after the photodamage and degradation of the D_1 protein of PSII under high light flux. To achieve the water-splitting capability, the newly functional OEC must be properly assembled after the repairing of the D_1 protein of PSII (Barber and Andersson, 1992; Dasgupta et al., 2008). In PSII, the early steps of the assembly of the OEC involving two Mn and one Ca ions have been studied for more than 50 years (Cheniae and Martin, 1971; Dasgupta et al., 2008; Bao and Burnap, 2016; Murray et al., 2020); on the other hand, the assembly of the third and the fourth Mn ions in OEC is fully unknown (Bao and Burnap, 2016; Avramov et al., 2020). Considering the observed thermodynamical stability of the fully carboxylic ligand coordinated Mn_3CaO_4-cluster (**5**) observed (Chen et al., 2022), we propose that a similar Mn_3CaO_4-cluster could be present during the synthesis of the OEC in PSII. If it was the case, a mono-nuclear Mn ion (similar to that in **6**) would be necessary to be incorporated into the Mn_3CaO_4-cluster, followed by structural rearrangements to form the intact OEC, as has been suggested recently (Gisriel et al., 2020; Sato et al., 2021).

LIGANDS SUBSTITUTED OEC'S MIMICS

In order to improve the stability of the artificial Mn_4CaO_4-cluster, we have optimized its peripheral environment by replacing the two pivalic acid molecules on the calcium with organic solvent molecules (Chen et al., 2019). Structures of two new Mn_4CaO_4-complexes, $[Mn_4CaO_4(^tBuCO_2)_8(Py)(^tBuCO_2H)(CH_3CN)]$ (**8**) and $[Mn_4CaO_4(^tBuCO_2)_8(Py)(DMF)_2]$ (**9**) are shown in **Figure 9**. Interestingly, we have found that the change of these ligands on calcium does not affect neither the Mn_4CaO_4 core nor the oxidation states of the four Mn ions, as shown in **Figure 9**. This observation demonstrates that both the geometric structure and the electronic structure of the artificial Mn_4CaO_4-cluster are relatively stable, which provides chemical insights into the reason why the oxygenic photosynthetic organisms have selected the Mn_4CaO_4-cluster as the key structural unit to build the OEC in natural photosynthesis (Barber, 2020). Furthermore, the same oxidation states of the four Mn ions in **4**, **7**, **8,** and **9** (**Figures 5**, **7**, **9**) further confirm the assignment of the oxidation stats of

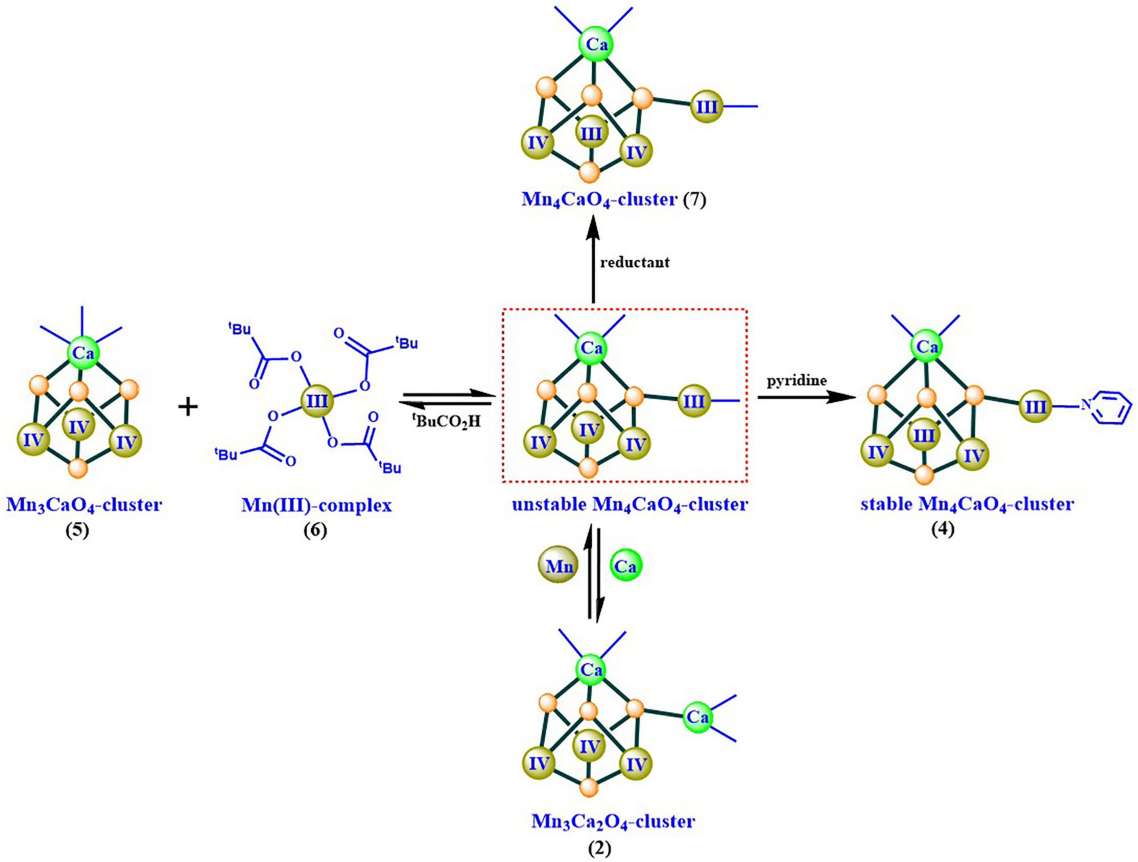

FIGURE 8 | Possible synthesizing mechanism of the artificial Mn_4CaO_4-cluster (**4**) (Chen et al., 2022).

(III, III, IV, IV) in the S_1 state OEC in PSII (Krewald et al., 2015).

CALCIUM SUBSTITUTED OEC'S MIMICS

The redox-inactive metal ion, Ca^{2+}, is an indispensable component for the catalytic function of the OEC, and its depletion results in the complete loss of the water-splitting capability of PSII (Yocum, 2008). In the biological system, Ca^{2+} can only be functionally replaced by Sr^{2+} (Boussac et al., 2004; Yocum, 2008). It has been argued that the Lewis acidity of the redox-inactive metal ion could play a role in modulating the redox potentials of heterometallic-oxide clusters (Tsui et al., 2013b; Tsui and Agapie, 2013; Krewald et al., 2016; Saito et al., 2021). However, the detailed functional role of the Ca^{2+} in the OEC remains largely unknown because direct investigation of the calcium is severely restricted by the lack of controlled modifications of this redox-inactive metal ion without changing the core structure and the local protein environment of the OEC in the biological system (Krewald et al., 2016; Saito et al., 2021).

To study the possible function of the calcium ion in OEC and to develop robust artificial catalysts for the water-splitting reaction, tremendous efforts have been devoted to preparing calcium substituted Mn_4XO_4-clusters in our laboratory. In 2021, we successfully prepared the $[Mn_4YO_4(^tBuCO_2)_9(Napy)]$ (Napy = 1,8-naphthyridine) (**10**) and $[Mn_4GdO_4(^tBuCO_2)_9(Napy)]$ (**11**) (Yao et al., 2021). Surprisingly, as shown in **Figure 10**, both the two rare-earth element-containing Mn_4XO_4-clusters (X = Y, Gd) have nearly the same core structure and peripheral carboxylic ligands, as well as the oxidation states of the four Mn ions as those in the Mn_4CaO_4-cluster (**4**) and in the S_1 state of the OEC (Umena et al., 2011). This observation clearly demonstrates that the substitution of the calcium by the rare-earth element does not affect neither the geometric structure nor the electronic structure of the Mn_4XO_4-clusters.

CV measurements (**Figure 11**) show that both Mn_4YO_4-cluster (**10**) and Mn_4GdO_4-cluster (**11**) have a redox potential of +0.79 V for the $[Mn^{III}_2Mn^{IV}_2]/[Mn^{III}Mn^{IV}_3]$ redox couple, which is nearly the same as that of the Mn_4CaO_4-cluster (**4**) (+0.8 V) (Zhang et al., 2015) and the estimated value for the $S_1 \rightarrow S_2$ transition ($\sim$ +0.8 V) of the OEC (Dau and Zaharieva, 2009; Mandal et al., 2020). Moreover, the redox potentials of −0.05 V and + 1.3 V for the $[Mn^{III}_3Mn^{IV}]/[Mn^{III}_2Mn^{IV}_2]$ and $[Mn^{III}Mn^{IV}_3]/[Mn^{IV}_4]$ irreversible redox couples can be estimated for both the Mn_4YO_4-cluster and the Mn_4GdO_4-cluster, respectively. These values are also close to that (−0.1 and + 1.25 V) observed in the Mn_4CaO_4-cluster (Zhang et al., 2015) as well. These results clearly show that the replacement of the calcium

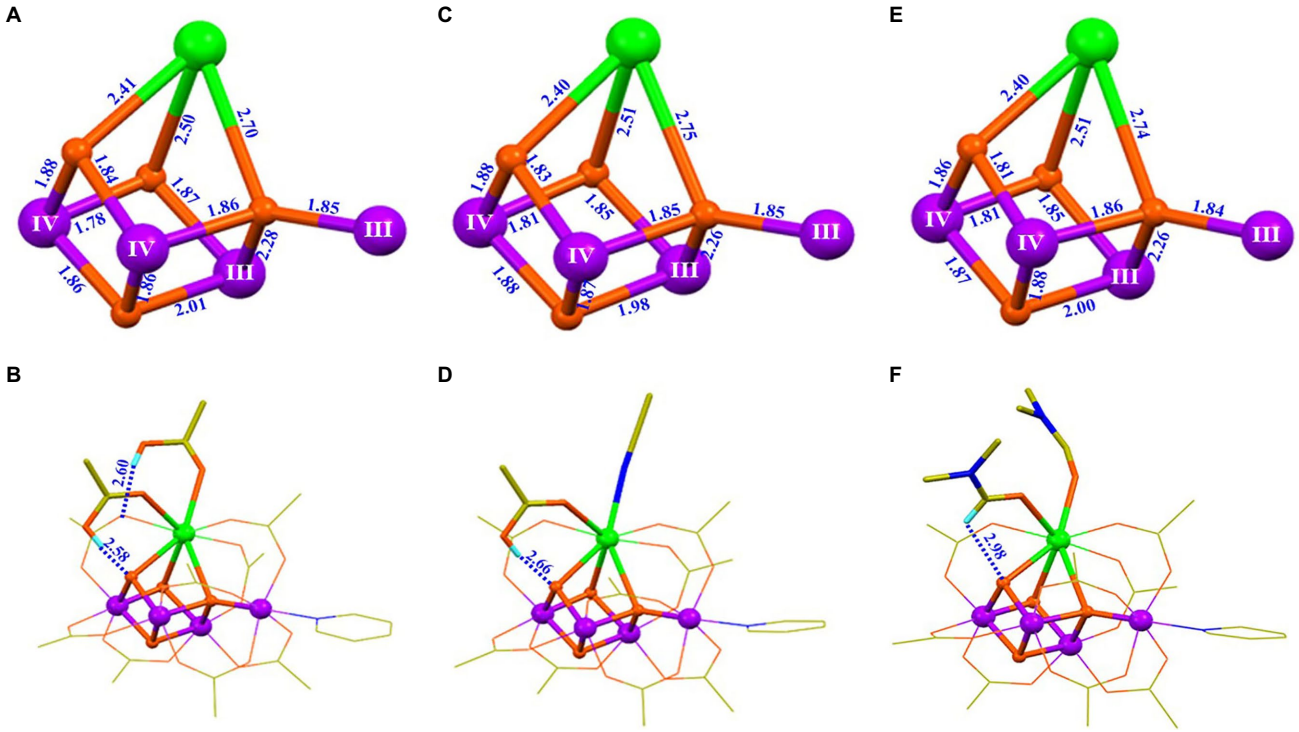

FIGURE 9 | Structural comparison of three artificial Mn_4CaO_4-complexes (**4**, **8**, **9**) (Zhang et al., 2015; Chen et al., 2019). **(A)** Core of **4**; **(B)** structure of **4**; **(C)** core of **8**; **(D)** structure of **8**; **(E)** core of **9**; **(F)** structure of **9**. All illustrations are the same as those in **Figure 5**.

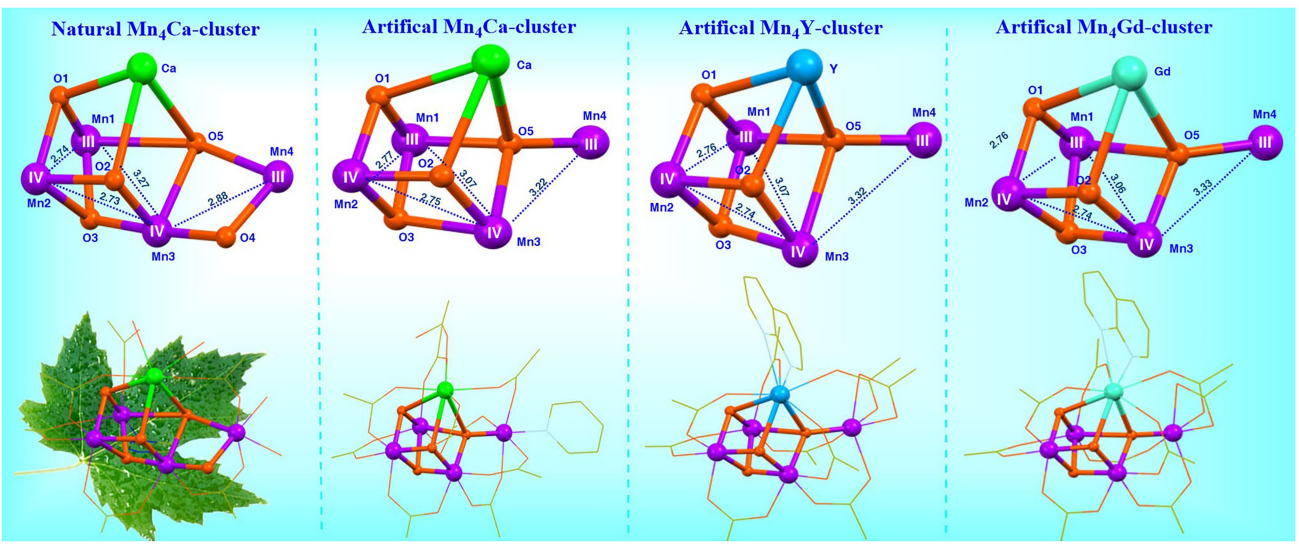

FIGURE 10 | Structural comparison of the OEC (Suga et al., 2015), Mn_4CaO_4-cluster (**4**) (Zhang et al., 2015), the Mn_4YO_4-cluster (**10**) and Mn_4GdO_4-cluster (**11**) (Yao et al., 2021). See **Figure 5** for further information.

by rare-earth element does not significantly affect redox potentials of the heterometallic-oxide Mn_4XO_4-cluster although the Lewis acidity of Y^{3+}, Gd^{3+}, and Ca^{2+} is significantly different. This observation challenges the earlier view that the redox-inactive metal ion would modulate the redox potentials of the heterometallic-oxide cluster (Tsui et al., 2013b; Tsui and Agapie, 2013).

The above results suggest that rare-earth elements can structurally and energetically replace the calcium in artificial neutral Mn_4XO_4 clusters in a chemical system, which, indeed,

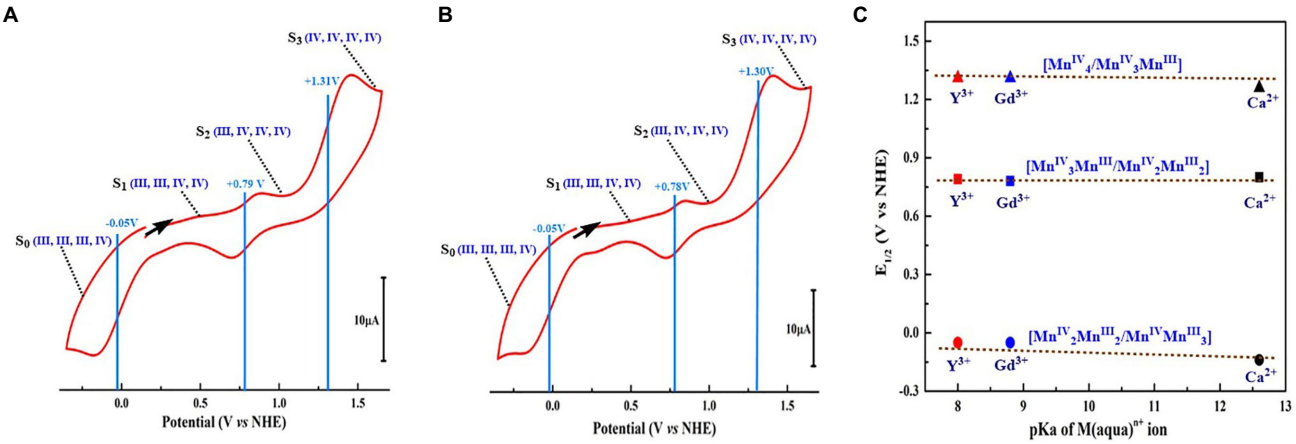

FIGURE 11 | Redox potentials of the Mn_4YO_4-cluster (**10**) and Mn_4GdO_4-cluster (**11**) (Yao et al., 2021). **(A)** CV of Mn_4YO_4-cluster. **(B)** CV of Mn_4GdO_4-cluster. The possible oxidation states of the four Mn ions are shown in blue. The scan direction is indicated by the arrow. **(C)** Dependence of E1/2 of three redox couples on pKa of the X(aqua)$^{n+}$ ion (Perrin, 1982) of three Mn4XO4-clusters. All potentials were referenced to NHE.

sheds new light on the functional role of the calcium in the OEC and supports the idea that the redox-inactive metal ion could indeed play roles in maintaining the cluster's integrity and stability instead of modulating the redox potential of the OEC. Obviously, these robust rare-earth element-containing Mn_4XO_4-clusters provide a structurally well-defined molecular platform to investigate the structure–function relationship of its biological paradigm and shed new light on the design of efficient water-splitting catalysts in artificial photosynthesis.

CHALLENGE FOR FUTURE MIMICKING

Although these Mn_4XO_4-clusters (X = Ca/Y/Gd) closely mimic the OEC in many aspects and provide new insights into the structure–function relationship of the biological catalyst, it remains a great challenge to overcome in order to discover a precise mimic of the structure and function of the OEC in a laboratory. In the first place, the μ_2-oxide bridge (O4) seen in the S_1 state of the OEC is still missing in all the current known Mn_4XO_4-clusters. Incorporating this last "missing puzzle" into artificial Mn_4XO_4-cluster is a great challenge for synthetic chemistry, which is urgently needed for the understanding of the functional role of this oxide bridge and of the catalytic mechanism for the O=O bond formation in the OEC. Further, all synthetic Mn_4XO_4-clusters display very poor solubility in aqueous solution because of the hydrophobic peripheral environment mainly provided by the pivalate groups (i. e. $^tBuCO_2$); thus, it is difficult to carry out its catalytic performance in aqueous solution as is the case with many other artificial catalysts reported thus far (Zhang and Sun, 2019b; Kondo et al., 2021). In addition, it has been found that many Mn complexes are not stable in the aqueous solution during the catalytic reaction (Hocking et al., 2011; Li et al., 2017); thus, it is crucial to develop a proper experimental condition for the catalytic performance of these OEC's mimics. In the biological system, the Mn_4CaO_5-cluster is surrounded by non-aqueous protein environment with special channels for the delivery of protons, electrons, and the substrate (Shen, 2015; Hussein et al., 2021). Obviously, mimicking the first and the second coordination spheres of the OEC in PSII with functional channels is further required to achieve high reactivity in the future.

CONCLUDING REMARKS

In summary, the crystallographic studies of PSII have revealed that the OEC is composed of an asymmetric Mn_4CaO_5-cluster; however, the detailed catalytic mechanism for the water-splitting reaction remains elusive due to the structural uncertainty of the different intermediate states of the OEC during its catalytic turnover. It is a great challenge to precisely mimic the OEC in the laboratory, yet a series of artificial Mn_4XO_4-clusters (X = Ca/Y/Gd) have been reported recently, which closely mimic both the geometric structure and the electronic structure, as well as the redox properties of the OEC in PSII. The investigation of these structurally well-defined chemical models provides distinct chemical insights into the understanding of the structure–function relationship of the OEC as well as the catalytic mechanism of the water-splitting reaction in natural photosynthesis. We list below several major take-home messages.

The oxidation states of the four Mn ions in all these Mn_4XO_4-clusters are (III, III, IV, IV), which provides the unambiguous chemical evidence for the "high-oxidation paradigm" assignment of the four Mn ions in the S_1 state of the OEC (Krewald et al., 2015).

The preparation and reactivity of artificial Mn_4CaO_4-clusters clearly demonstrate that this cluster is thermodynamically stable, which supports the proposal that the Mn_4CaO_4-cluster could be an evolutionary origin of the natural OEC (Barber, 2016).

The finding that the rare-earth elements can structurally and energetically replace the calcium in the Mn_4CaO_4-cluster provides important chemical insight into the functional role of the calcium in the OEC. It indicates that the redox-inactive metal ion could play roles in maintaining the cluster's integrity and stability instead of modulating the redox potential of the OEC.

Based on the characterization of artificial Mn_4XO_4-clusters, we clearly see that all μ_3- and μ_4- oxide bridges are tightly bound to the cluster, supporting that they may play roles in maintaining the cluster's stability and integrity rather than as reactive sites for the O=O bond formation. However, we should point out that precise structural mimicking and functional mimicking are urgently required in the future to reveal the detailed catalytic mechanism and to achieve the high reactivity of water-splitting reaction in artificial photosynthesis. We believe that the further investigation of these robust artificial Mn_4XO_4-clusters would help to develop efficient man-made catalysts for the water-splitting reaction in artificial photosynthesis.

AUTHOR CONTRIBUTIONS

CZ conceived the project and designed experiments. YC carried out BVS calculation. CZ, CC, BX, and RY participated in the synthesis and characterization of artificial Mn_4XO_4-clusters involved in the paper. YC and CZ wrote the manuscript All authors contributed to the article and approved the submitted version.

FUNDING

This work was supported by the National Natural Science Foundation of China (Nos. 91961203 and 22001255), the National Key Research & Development Program of China (No. 2017YFA0503704), the Strategic Priority Research Program of the Chinese Academy of Sciences (Nos. XDA21010212 and XDB17030600), and the Youth Innovation Promotion Association CAS (No. 2022030).

REFERENCES

Amin, M., Badawi, A., and Obayya, S. S. (2016). Radiation damage in XFEL: case study from the oxygen-evolving complex of photosystem II. *Sci. Rep.* 6:36492. doi: 10.1038/srep36492

Andreiadis, E. S., Chavarot-Kerlidou, M., Fontecave, M., and Artero, V. (2011). Artificial photosynthesis: from molecular catalysts for light-driven water splitting to photoelectrochemical cells. *Photochem. Photobiol.* 87, 946–964. doi: 10.1021/acs.accounts.6b00405

Askerka, M., Brudvig, G. W., and Batista, V. S. (2017). The O_2-evolving complex of photosystem II: recent insights from quantum mechanics/molecular mechanics (QM/MM), extended X-ray absorption fine structure (EXAFS), and femtosecond X-ray crystallography data. *Acc. Chem. Res.* 50, 41–48. doi: 10.1021/acs.biochem.5b00089

Askerka, M., Vinyard, D. J., Wang, J., Brudvig, G. W., and Batista, V. S. (2015). Analysis of the radiation-damage-free X-ray structure of photosystem II in light of EXAFS and QM/MM data. *Biochemistry* 54, 1713–1716. doi: 10.1021/acs.biochem.5b00089

Avramov, A. P., Hwang, H. J., and Burnap, R. L. (2020). The role of Ca^{2+} and protein scaffolding in the formation of nature's water oxidizing complex. *Proc. Natl. Acad. Sci. U. S. A.* 117, 28036–28045. doi: 10.1073/pnas.2011315117

Bao, H., and Burnap, R. L. (2016). Photoactivation: The light-driven assembly of the water oxidation complex of photosystem II. *Front. Plant Sci.* 7:578. doi: 10.3389/fpls.2016.00578

Barber, J. (2009). Photosynthetic energy conversion: natural and artificial. *Chem. Soc. Rev.* 38, 185–196. doi: 10.1039/b802262n

Barber, J. (2016). Mn_4Ca cluster of photosynthetic oxygen-evolving center: structure, function and evolution. *Biochemistry* 55, 5901–5906. doi: 10.1021/acs.biochem.6b00794

Barber, J. (2017). A mechanism for water splitting and oxygen production in photosynthesis. *Nat. Plants* 3:17041. doi: 10.1038/nplants.2017.41

Barber, J. (2020). Solar-driven water-splitting provides a solution to the energy problem underpinning climate change. *Biochem. Soc. Trans.* 48, 2865–2874. doi: 10.1042/BST20200758

Barber, J., and Andersson, B. (1992). Too much of good things: light can be bad for photosynthesis. *Trends Biochem. Sci.* 17, 61–66. doi: 10.1126/science.1200165

Blankenship, R. E. (2021). *Molecular Mechanisms of Photosynthesis*. Malden, USA: Blackwell Science Ltd.

Blankenship, R. E., Tiede, D. M., Barber, J., Brudvig, G. W., Fleming, G., Ghirardi, M., et al. (2011). Comparing photosynthetic and photovoltaic efficiencies and recognizing the potential for improvement. *Science* 332, 805–809. doi: 10.1126/science.1200165

Boussac, A., Rappaport, F., Carrier, P., Verbavatz, J. M., Gobin, R., Kirilovsky, D., et al. (2004). Biosynthetic Ca^{2+}/Sr^{2+} exchange in the photosystem II oxygen-evolving enzyme of *Thermosynechococcus elongatus*. *J. Biol. Chem.* 279, 22809–22819. doi: 10.1074/jbc.M401677200

Britt, R. D., and Marchiori, D. A. (2019). Photosystem II, poised for O_2 formation. *Science* 366, 305–306. doi: 10.1126/science.aaz4522

Brown, I. D. (2009). Recent developments in the methods and applications of the bond valence model. *Chem. Rev.* 109, 6858–6919. doi: 10.1021/cr900053k

Capone, M., Narzi, D., and Guidoni, L. (2021). Mechanism of oxygen evolution and Mn_4CaO_5 cluster restoration in the natural water-oxidizing catalyst. *Biochemistry* 60, 2341–2348. doi: 10.1021/acs.biochem.1c00226

Cardona, T., Sedoud, A., Cox, N., and Rutherford, A. W. (2012). Charge separation in photosystem II: A comparative and evolutionary overview. *Biochim. Biophys. Acta* 1817, 26–43. doi: 10.1016/j.bbabio.2011.07.012

Chang, W., Chen, C., Dong, H., and Zhang, C. (2017). Artificial Mn_4-oxido complexes mimic the oxygen-evolving center in photosynthesis. *Sci. Bull.* 62, 665–668. doi: 10.1016/j.scib.2017.04.005

Chen, C., Chen, Y., Yao, R., Li, Y., and Zhang, C. (2019). Artificial Mn_4Ca clusters with exchangeable solvent molecules mimicking the oxygen-evolving center in photosynthesis. *Angew. Chem. Int. Ed.* 58, 3939–3942. doi: 10.1002/anie.201814440

Chen, Q. F., Guo, Y. H., Yu, Y. H., and Zhang, M. T. (2021). Bioinspired molecular clusters for water oxidation. *Coord. Chem. Rev.* 448:214164. doi: 10.1016/j.ccr.2021.214164

Chen, C., Li, Y., Zhao, G., Yao, R., and Zhang, C. (2017). Natural and artificial Mn_4Ca cluster for the water splitting reaction. *Chem. Sus. Chem* 10, 4403–4408. doi: 10.1002/cssc.201701371

Chen, C., Xu, B., Yao, R., Chen, Y., and Zhang, C. (2022). Synthesizing mechanism of the Mn_4Ca-cluster mimicking the oxygen-evolving center in photosynthesis. *Chem. Sus. Chem.* 15:e202102661. doi: 10.1002/cssc.202102661

Chen, C., and Zhang, C. (2021). Mn_4Ca-cluster: photosynthetic water-splitting catalyst. *Comprehensive Coordination Chemistry III* 2, 454–465. doi: 10.1016/B978-0-12-409547-2.14830-9

Chen, C., Zhang, C., Dong, H., and Zhao, J. (2014). A synthetic model for the oxygen-evolving complex in Sr^{2+}-containing photosystem II. *Chem. Commun.* 50, 9263–9265. doi: 10.1039/c4cc02349h

Chen, C., Zhang, C., Dong, H., and Zhao, J. (2015). Artificial synthetic $Mn^{IV}Ca$-oxido complexes mimic the oxygen-evolving complex in photosystem II. *Dalton Trans.* 44, 4431–4435. doi: 10.1039/c4dt03459g

Cheniae, G. M., and Martin, I. F. (1971). Photoactivation of the manganese catalyst of O_2 evolution. I. Biochemical and kinetic aspects. *Biochim. Biophys. Acta* 253, 167–181. doi: 10.1016/0005-2728(71)90242-8

Concepcion, J. J., House, R. L., Papanikolas, J. M., and Meyer, T. J. (2012). Chemical approaches to artificial photosynthesis. *Proc. Natl. Acad. Sci. U. S. A.* 109, 15560–15564. doi: 10.1073/pnas.1212254109

Corry, T. A., and O'Malley, P. J. (2018). Evidence of O-O bond formation in the final metastable S_3 state of nature's water oxidizing complex implying a novel mechanism of water oxidation. *J. Phys. Chem. Lett.* 9, 6269–6274. doi: 10.1021/acs.jpclett.8b02793

Cox, N., Pantazis, D. A., and Lubitz, W. (2020). Current understanding of the mechanism of water oxidation in photosystem II and its relation to XFEL data. *Annu. Rev. Biochem.* 89, 795–820. doi: 10.1146/annurev-biochem-011520104801

Cox, N., Pantazis, D. A., Neese, F., and Lubitz, W. (2014a). Biological water oxidation. *Acc. Chem. Res.* 46, 1588–1596. doi: 10.1021/ar3003249

Cox, N., Retegan, M., Neese, F., Pantazis, D. A., Boussac, A., and Lubitz, W. (2014b). Electronic structure of the oxygen-evolving complex in photosystem II prior to O-O bond formation. *Science* 345, 804–808. doi: 10.1126/science.1254910

Dasgupta, J., Ananyev, G. M., and Dismukes, G. C. (2008). Photoassembly of the water-oxidizing complex in photosystem II. *Coord. Chem. Rev.* 252, 347–360. doi: 10.1016/j.ccr.2007.08.022

Dau, H., Grundmeier, A., Loja, P., and Haumann, M. (2008). On the structure of the manganese complex of photosystem II: extended-range EXAFS data and specific atomic-resolution models for four S-states. *Phil. Trans. R. Soc. Lond. B* 363, 1237–1244. doi: 10.1098/rstb.2007.2220

Dau, H., and Haumann, M. (2007). Eight steps preceding O-O bond formation in oxygenic photosynthesis—A basic reaction cycle of the photosystem II manganese complex. *Biochim. Biophys. Acta* 1767, 472–483. doi: 10.1016/j.bbabio.2007.02.022

Dau, H., and Haumann, M. (2008). The manganese complex of photosystem II in its reaction cycle—basic framework and possible realization at the atomic level. *Coord. Chem. Rev.* 252, 273–295. doi: 10.1016/j.ccr.2007.09.001

Dau, H., and Zaharieva, I. (2009). Principles, efficiency and blueprint character of solar-energy conversion in photosynthetic water oxidation. *Acc. Chem. Res.* 42, 1861–1870. doi: 10.1021/ar900225y

Davis, K. M., and Pushkar, Y. N. (2015). Structure of the oxygen evolving complex of photosystem II at room temperature. *J. Phys. Chem. B* 119, 3492–3498. doi: 10.1021/acs.jpcb.5b00452

Davis, K. M., Sullivan, B. T., Palenik, M. C., Yan, L., Purohit, V., Robison, G., et al. (2018). Rapid evolution of the photosystem II electronic structure during water splitting. *Phys. Rev. X.* 8:041014. doi: 10.1103/PhysRevX.8.041014

Debus, R. J. (1992). The manganese and calcium ions of photosynthetic oxygen evolution. *Biochim. Biophys. Acta* 1102, 269–352. doi: 10.1016/0167-4838(92)90520-N

Diner, B. A., and Britt, R. D. (2005). "The redox-active Tyrosines YZ and YD," in *Photosystem II: The Light-Driven Water: Plastoquinone Oxidoreductase*. eds. T. J. Wydrzynski and K. Satoh (Dordrecht, The Netherlands: Springer), 207–233.

Dismukes, G. C., Brimblecombe, R., Felton, G. A. N., Pryadun, R. S., Sheats, J. E., Spiccia, L., et al. (2009). Development of bioinspired Mn_4O_4-cubane water oxidation catalysts: lessons from photosynthesis. *Acc. Chem. Res.* 42, 1935–1943. doi: 10.1021/ar900249x

El-Khouly, M. E., El-Mohsnawy, E., and Fukuzumi, S. (2017). Solar energy conversion: From natural to artificial photosynthesis. *J Photochem Photobiol C: Photochem Rev* 31, 36–83. doi: 10.1016/j.jphotochemrev.2017.02.001

Ezhov, R., Ravari, A. K., Bury, G., Smith, P. F., and Pushkar, Y. (2021). Do multinuclear 3d metal catalysts achieve O–O bond formation via radical coupling or via water nucleophilic attack? WNA leads the way in $[Co_4O_4]^{n+}$. *Chem Catalysis* 1, 407–422. doi: 10.1016/j.checat.2021.03.013

Faunce, T. A., Lubitz, W., Rutherford, A. W., MacFarlane, D., Moore, G. F., Yang, P., et al. (2013). Energy and environment policy case for a global project on artificial photosynthesis. *Energy Environ. Sci.* 6, 695–698. doi: 10.1039/c3ee00063j

Ferreira, K. N., Iverson, T. M., Maghlaoui, K., Barber, J., and Iwata, S. (2004). Architecture of the photosynthetic oxygen-evolving center. *Science* 303, 1831–1838. doi: 10.1126/science.1093087

Gatt, P., Petrie, S., Stranger, R., and Pace, R. J. (2012). Rationalizing the 1.9 Å crystal structure of photosystem II — A remarkable Jahn-teller balancing act induced by a single proton transfer. *Angew. Chem. Int. Ed.* 51, 12025–12028. doi: 10.1002/anie.201206316

Gerey, B., Goure, E., Fortage, J., Pecaut, J., and Collomb, M. N. (2016). Manganese-calcium/strontium heterometallic compounds and their relevance for the oxygen-evolving center of photosystem II. *Coord. Chem. Rev.* 319, 1–24. doi: 10.1016/j.ccr.2016.04.002

Gisriel, C. J., Wang, J., Liu, J., Flesher, D. A., Reiss, K. M., Huang, H. L., et al. (2022). High-resolution cryo-electron microscopy structure of photosystem II from the mesophilic cyanobacterium, Synechocystis sp. PCC 6803. *Proc. Natl. Acad. Sci. U. S. A.* 119:e2116765118. doi: 10.1073/pnas.2116765118

Gisriel, C. J., Zhou, K., Huang, H. L., Debus, R. J., Xiong, Y., and Brudvig, G. W. (2020). Cryo-EM structure of monomeric photosystem II from *synechocystis sp.* PCC 6803 lacking the water-oxidation complex. *Joule* 4, 2131–2148. doi: 10.1016/j.joule.2020.07.016

Govindjee, G., Shevela, D., and Björn, L. O. (2017). Evolution of the Z-scheme of photosynthesis: a perspective. *Photosyn. Res.* 133, 5–15. doi: 10.1007/s11120-016-0333-z

Grabolle, M., Haumann, M., Müller, C., Liebisch, P., and Dau, H. (2006). Rapid loss of structural motifs in the manganese complex of oxygenic photosynthesis by X-ray irradiation at 10-300K. *J. Biol. Chem.* 281, 4580–4588. doi: 10.1074/jbc.M509724200

Graça, A. T., Hall, M., Persson, K., and Schröder, W. P. (2021). High-resolution model of Arabidopsis photosystem II reveals the structural consequences of digitonin-extraction. *Sci. Rep.* 11:15534. doi: 10.1038/s41598-021-94914-x

Guskov, A., Kern, J., Gabdulkhakov, A., Broser, M., Zouni, A., and Saenger, W. (2009). Cyanobacterial photosystem II at 2.9-Å resolution and the role of quinones, lipids, channels and chloride. *Nat. Struct. Mol. Biol.* 16, 334–342. doi: 10.1038/nsmb.1559

Gust, D., Moore, T. A., and Moore, A. L. (2010). Solar fuels via artificial photosynthesis. *Acc. Chem. Res.* 42, 1890–1898. doi: 10.1021/ar900209b

Haumann, M., Liebisch, P., Muller, C., Barra, M., Grabolle, M., and Dau, H. (2005). Photosynthetic O_2 formation tracked by time-resolved x-ray experiments. *Science* 310, 1019–1021. doi: 10.1126/science.1117551

Herrero, C., Lassalle-Kaiser, B., Leibl, W., Rutherford, A. W., and Aukauloo, A. (2008). Artificial systems related to light driven electron transfer processes in PSII. *Coord. Chem. Rev.* 252, 456–468. doi: 10.1016/j.ccr.2007.09.002

Hocking, R. K., Brimblecombe, R., Chang, L. Y., Singh, A., Cheah, M. H., Glover, C., et al. (2011). Water-oxidation catalysis by manganese in a geochemical-like cycle. *Nat. Chem.* 3, 461–466. doi: 10.1038/NCHEM.1049

Hunter, B. M., Gray, H. B., and Müller, A. M. (2016). Earth-abundant heterogeneous water oxidation catalysts. *Chem. Rev.* 116, 14120–14136. doi: 10.1021/acs.chemrev.6b00398

Hussein, R., Ibrahim, M., Bhowmick, A., Simon, P. S., Chatterjee, R., Lassalle, L., et al. (2021). Structural dynamics in the water and proton channels of photosystem II during the S_2 to S_3 transition. *Nat. Commun.* 12:6531. doi: 10.1038/s41467-021-26781-z

Ibrahim, M., Fransson, T., Chatterjee, R., Cheah, M. H., Hussein, R., Lassalle, L., et al. (2020). Untangling the sequence of events during the $S_2 \rightarrow S_3$ transition in photosystem II and implications for the water oxidation mechanism. *Proc. Natl. Acad. Sci. U. S. A.* 117, 12624–12635. doi: 10.1073/pnas.2000529117

Junge, W. (2019). Oxygenic photosynthesis: history, status and perspective. *Q. Rev. Biophys.* 52:e1. doi: 10.1017/S0033583518000112

Kamiya, N., and Shen, J. R. (2003). Crystal structure of oxygen-evolving photosystem II from *Thermosynechococcus vulcanus* at 3.7 Å resolution. *Proc. Natl. Acad. Sci. U. S. A.* 100, 98–103. doi: 10.1073/pnas.0135651100

Kanady, J. S., Lin, P. H., Carsch, K. M., Nielsen, R. J., Takase, M. K., Goddard, W. A., et al. (2014). Toward models for the full oxygen-evolving complex of photosystem II by ligand coordination to lower the symmetry of the Mn_3CaO_4 cubane: demonstration that electronic effects facilitate binding of a fifth metal. *J. Am. Chem. Soc.* 136, 14373–14376. doi: 10.1021/ja508160x

Kanady, J. S., Tsui, E. Y., Day, M. W., and Agapie, T. (2011). A synthetic model of the Mn_3Ca subsite of the oxygen-evolving complex in photosystem II. *Science* 333, 733–736. doi: 10.1126/science.1206036

Kärkäs, M. D., Verho, O., Johnston, E. V., and Åkermark, B. (2014). Artificial photosynthesis: molecular systems for catalytic water oxidation. *Chem. Rev.* 114, 11863–12001. doi: 10.1021/cr400572f

Kato, K., Miyazaki, N., Hamaguchi, T., Nakajima, Y., Akita, F., Yonekura, K., et al. (2021). High-resolution cryo-EM structure of photosystem II reveals

damage from high-dose electron beams. *Commun. Biol.* 4:382. doi: 10.1038/s42003-021-01919-3

Kawashima, K., Takaoka, T., Kimura, H., Saito, K., and Ishikita, H. (2018). O_2 evolution and recovery of the water-oxidizing enzyme. *Nat. Commun.* 9:1247. doi: 10.1038/s41467-018-03545-w

Kern, J., Chatterjee, R., Young, I. D., Fuller, F. D., Lassalle, L., Ibrahim, M., et al. (2018). Structures of the intermediates of Kok's photosynthetic water oxidation clock. *Nature* 563, 421–425. doi: 10.1038/s41586-018-0681-2

Kok, B., Forbush, B., and McGloin, M. (1970). Cooperation of charges in photosynthetic O_2 evolution. I. A linear four step mechanism. *Photochem. Photobiol.* 11, 457–475. doi: 10.1111/j.1751-1097.1970.tb06017.x

Kondo, M., Tatewaki, H., and Masaoka, S. (2021). Design of molecular water oxidation catalysts with earth-abundant metal ions. *Chem. Soc. Rev.* 50, 6790–6831. doi: 10.1039/d0cs01442g

Koua, F. H. M., Umena, Y., Kawakami, K., and Shen, J. R. (2013). Structure of Sr-substituted photosystem II at 2.1 Å resolution and its implications in the mechanism of water oxidation. *Proc. Natl. Acad. Sci. U. S. A.* 110, 3889–3894. doi: 10.1073/pnas.1219922110

Krewald, V., Neese, F., and Pantazis, D. A. (2016). Redox potential tuning by redox-inactive cations in nature's water oxidizing catalyst and synthetic analogues. *Phys. Chem. Chem. Phys.* 18, 10739–10750. doi: 10.1039/c5cp07213a

Krewald, V., Retegan, M., Cox, N., Messinger, J., Lubitz, W., DeBeer, S., et al. (2015). Metal oxidation states in biological water splitting. *Chem. Sci.* 6, 1676–1695. doi: 10.1039/c4sc03720k

Kupitz, C., Basu, S., Grotjohann, I., Fromme, R., Zatsepin, N. A., Rendek, K. N., et al. (2014). Serial time-resolved crystallography of photosystem II using a femtosecond X-ray laser. *Nature* 513, 261–265. doi: 10.1038/nature13453

Li, J., Güttinger, R., Moré, R., Song, F., Wan, W., and Patzke, G. R. (2017). Frontiers of water oxidation: the quest for true catalysts. *Chem. Soc. Rev.* 46, 6124–6147. doi: 10.1039/c7cs00306d

Li, X. C., Li, J., and Siegbahn, P. E. M. (2020a). A theoretical study of the recently suggested Mn^{VII} mechanism for O-O bond formation in photosystem II. *J. Phys. Chem. A* 124, 8011–8018. doi: 10.1021/acs.jpca.0c05135

Li, H., Nakajima, Y., Nomura, T., Sugahara, M., Yonekura, S., Chan, S. K., et al. (2021). Capturing structural changes of the S_1 to S_2 transition of photosystem II using time-resolved serial femtosecond crystallography. *IUCrJ* 8, 431–443. doi: 10.1107/S2052252521002177

Li, Y., Yao, R., Chen, Y., Xu, B., Chen, C., and Zhang, C. (2020b). Mimicking the catalytic center for the water-splitting reaction in photosystem II. *Catalysts* 10:185. doi: 10.3390/catal10020185

Limburg, J., Vrettos, J. S., Liable-Sands, L. M., Rheingold, A. L., Crabtree, R. H., and Brudvig, G. W. (1999). A functional model for O-O bond formation by the O_2-evolving complex in photosystem II. *Science* 283, 1524–1527. doi: 10.1126/science.283.5407.1524

Lin, P. H., Takase, M. K., and Agapie, T. (2015). Investigations of the effect of the non-manganese metal in heterometallic-oxido cluster models of the oxygen evolving complex of photosystem II: lanthanides as substitutes for calcium. *Inorg. Chem.* 54, 59–64. doi: 10.1021/ic5015219

Lionetti, D., Suseno, S., Tsui, E. Y., Lu, L., Stich, T. A., Carsch, K. M., et al. (2019). Effects of Lewis acidic metal ions (M) on oxygen-atom transfer reactivity of heterometallic Mn_3MO_4 cubane and $Fe_3MO(OH)$ and $Mn_3MO(OH)$ clusters. *Inorg. Chem.* 58, 2336–2345. doi: 10.1021/acs.inorgchem.8b02701

Loll, B., Kern, J., Saenger, W., Zouni, A., and Biesiadka, J. (2005). Towards complete cofactor arrangement in the 3.0Å resolution structure of photosystem II. *Nature* 438, 1040–1044. doi: 10.1038/nature04224

Lubitz, W., Chrysina, M., and Cox, N. (2019). Water oxidation in photosystem II. *Photosynth. Res.* 142, 105–125. doi: 10.1007/s11120-019-00648-3

Mandal, M., Kawashima, K., Saito, K., and Ishikita, H. (2020). Redox potential of the oxygen-evolving complex in the electron transfer cascade of photosystem II. *J. Phys. Chem. Lett.* 11, 249–255. doi: 10.1021/acs.jpclett.9b02831

Marchiori, D. A., Debus, R. J., and Britt, R. D. (2020). Pulse EPR spectroscopic characterization of the S_3 state of the oxygen-evolving complex of photosystem II isolated from synechocystis. *Biochemistry* 59, 4864–4872. doi: 10.1021/acs.biochem.0c00880

Mukherjee, S., Stull, J. A., Yano, J., Stamatatos, T. C., Pringouri, K., Stich, T. A., et al. (2012). Synthetic model of the asymmetric $[Mn_3CaO_4]$ cubane core of the oxygen-evolving complex of photosystem II. *Proc. Natl. Acad. Sci. U. S. A.* 109, 2257–2262. doi: 10.1073/pnas.1115290109

Mukhopadhyay, S., Mandal, S. K., Bhaduri, S., and Armstrong, W. H. (2004). Manganese clusters with relevance to photosystem II. *Chem. Rev.* 104, 3981–4026. doi: 10.1021/cr0206014

Mullins, C. S., and Pecoraro, V. L. (2008). Reflections on small molecule manganese models that seek to mimic photosynthetic water oxidation chemistry. *Coord. Chem. Rev.* 252, 416–443. doi: 10.1016/j.ccr.2007.07.021

Murray, J. W., Rutherford, A. W., and Nixon, P. J. (2020). Photosystem II in a state of disassembly. *Joule* 4, 2082–2084. doi: 10.1016/j.joule.2020.09.014

Najafpour, M. M., Renger, G., Hołynska, M., Moghaddam, A. N., Aro, E. M., Carpentier, R., et al. (2016). Manganese compounds as water-oxidizing catalysts: from the natural water-oxidizing complex to nanosized manganese oxide structures. *Chem. Rev.* 116, 2886–2936. doi: 10.1021/acs.chemrev.5b00340

Nocera, D. G. (2017). Solar fuels and solar chemicals industry. *Acc. Chem. Res.* 50, 616–619. doi: 10.1021/acs.accounts.6b00615

Pace, R. J., Jin, L., and Stranger, R. (2012). What spectroscopy reveals concerning the Mn oxidation levels in the oxygen evolving complex of photosystem II: X-ray to near infra-red. *Dalton Trans.* 41, 11145–11160. doi: 10.1039/c2dt30938f

Pantazis, D. A. (2018). Missing pieces in the puzzle of biological water oxidation. *ACS Catal.* 8, 9477–9507. doi: 10.1021/acscatal.8b01928

Pantazis, D. A., Ames, W., Cox, N., Lubitz, W., and Neese, F. (2012). Two interconvertible structures that explain the spectroscopic properties of the oxygen-evolving complex of photosystem II in the S_2 state. *Angew. Chem. Int. Ed.* 51, 9935–9940. doi: 10.1002/anie.201204705

Paul, S., Neese, F., and Pantazis, D. A. (2017). Structural models of the biological oxygen-evolving complex: achievements, insights, and challenges for biomimicry. *Green Chem.* 19, 2309–2325. doi: 10.1039/c7gc00425g

Pecoraro, V. L., Baldwin, M. J., Caudle, M. T., Hsieh, W. Y., and Law, N. A. (1998). A proposal for water oxidation in photosystem II. *Pure Appl. Chem.* 70, 925–929. doi: 10.1351/pac199870040925

Peloquin, J. M., and Britt, R. D. (2001). EPR/ENDOR characterization of the physical and electronic structure of the OEC Mn-cluster. *Biochim. Biophys. Acta* 1503, 96–111. doi: 10.1016/S0005-2728(00)00219-X

Perrin, D. D. (1982). *Ionisation Constants of Inorganic Acids and Bases in Aqueous Solution*. Oxford: Pergamon Press.

Petrie, S., Terrett, R., Stranger, R., and Pace, R. J. (2020). Rationalizing the geometries of the water oxidising complex in the atomic resolution, nominal S_3 state crystal structures of photosystem II. *ChemPhysChem* 21, 785–801. doi: 10.1002/cphc.201901106

Petrouleas, V., and Crofts, A. R. (2005). "The iron-quinone acceptor complex," in *Photosystem II: The light-driven water: Plastoquinone Oxidoreductase*. eds. T. J. Wydrzynski and K. Satoh (Dordrecht, The Netherlands: Springer), 177–206.

Pushkar, Y., Davis, K. M., and Palenik, M. C. (2018). Model of the oxygen evolving complex which is highly predisposed to O-O bond formation. *J. Phys. Chem. Lett.* 9, 3525–3531. doi: 10.1021/acs.jpclett.8b00800

Rappaport, F., and Diner, B. A. (2008). Primary photochemistry and energetics leading to the oxidation of the Mn_4Ca cluster and to the evolution of molecular oxygen in photosystem II. *Coord. Chem. Rev.* 252, 259–272. doi: 10.1016/j.ccr.2007.07.016

Renger, G., and Holzwarth, A. R. (2005). "Primary electron transfer," in *Photosystem II: The light-driven water: Plastoquinone Oxidoreductase*. eds. T. J. Wydrzynski and K. Satoh (Dordrecht, The Netherlands: Springer), 139–175.

Saito, K., Nakagawa, M., Mandal, M., and Ishikita, H. (2021). Role of redox-inactive metals in controlling the redox potential of heterometallic manganese-oxido clusters. *Photosynth. Res.* 148, 153–159. doi: 10.1007/s11120-021-00846-y

Sato, A., Nakano, Y., Nakamura, S., and Noguchi, T. (2021). Rapid-scan time-resolved ATR-FTIR study on the photoassembly of the water-oxidizing Mn_4CaO_5 cluster in photosystem II. *J. Phys. Chem. B* 125, 4031–4045. doi: 10.1021/acs.jpcb.1c01624

Shen, J. R. (2015). The structure of photosystem II and the mechanism of water oxidation in photosynthesis. *Annu. Rev. Plant Biol.* 66, 23–48. doi: 10.1146/annurev-arplant-050312-120129

Shevela, D., Bjorn, L., and Govindjee, G. (2019). *Photosynthesis: Solar Energy for Life*. Singapore: World Scientific.

Shevela, D., Eaton-Rye, J. J., Shen, J. R., and Govindjee, G. (2012). Photosystem II and the unique role of bicarbonate: A historical perspective. *Biochim. Biophys. Acta* 1817, 1134–1151. doi: 10.1016/j.bbabio.2012.04.003

Shevela, D., Kern, J. F., Govindjee, G., Whitmarsh, J., and Messinger, J. (2021). *Photosystem II. Encyclopedia of Life Sciences*. Hoboken: Wiley.

Siegbahn, P. E. M. (2013). Water oxidation mechanism in photosystem II, including oxidations, proton release pathways, O-O bond formation and O_2 release. *Biochim. Biophys. Acta* 1827, 1003–1019. doi: 10.1016/j.bbabio.2012.10.006

Siegbahn, P. E. M. (2017). Nucleophilic water attack is not a possible mechanism for O-O bond formation in photosystem II. *Proc. Natl. Acad. Sci. U. S. A.* 114, 4966–4968. doi: 10.1073/pnas.1617843114

Styring, S., Sjöholm, J., and Mamedov, F. (2012). Two tyrosines that changed the world: interfacing the oxidizing power of photochemistry to water splitting in photosystem II. *Biochim. Biophys. Acta* 1817, 76–87. doi: 10.1016/j.bbabio.2011.03.016

Suga, M., Akita, F., Hirata, K., Ueno, G., Murakami, H., Nakajima, Y., et al. (2015). Native structure of photosystem II at 1.95Å resolution revealed by a femtosecond X-ray laser. *Nature* 517, 99–103. doi: 10.1038/nature13991

Suga, M., Akita, F., Sugahara, M., Kubo, M., Nakajima, Y., Nakane, T., et al. (2017). Light-induced structural changes and the site of O=O bond formation in PSII caught by XFEL. *Nature* 543, 131–135. doi: 10.1038/nature21400

Suga, M., Akita, F., Yamashita, K., Nakajima, Y., Ueno, G., Li, H., et al. (2019). An oxyl/oxo mechanism for oxygen-oxygen coupling in PSII revealed by an x-ray free-electron laser. *Science* 366, 334–338. doi: 10.1126/science.aax6998

Tanaka, A., Fukushima, Y., and Kamiya, N. (2017). Two different structures of the oxygen-evolving complex in the same polypeptide frameworks of photosystem II. *J. Am. Chem. Soc.* 139, 1718–1721. doi: 10.1021/jacs.6b09666

Tommos, C., and Babcock, G. T. (1998). Oxygen production in nature: A light-driven metalloradical enzyme process. *Acc. Chem. Res.* 31, 18–25. doi: 10.1021/ar9600188

Tsui, E. Y., and Agapie, T. (2013). Reduction potentials of heterometallic manganese–oxido cubane complexes modulated by redox-inactive metals. *Proc. Natl. Acad. Sci. U. S. A.* 110, 10084–10088. doi: 10.1073/pnas.1302677110

Tsui, E. Y., Kanady, J. S., and Agapie, T. (2013a). Synthetic cluster models of biological and heterogeneous manganese catalysts for O_2 evolution. *Inorg. Chem.* 52, 13833–13848. doi: 10.1021/ic402236f

Tsui, E. Y., Tran, R., Yano, J., and Agapie, T. (2013b). Redox-inactive metals modulate the reduction potential in heterometallic manganese-oxido clusters. *Nat. Chem.* 5, 293–299. doi: 10.1038/nchem.1578

Umena, Y., Kawakami, K., Shen, J. R., and Kamiya, N. (2011). Crystal structure of oxygen-evolving photosystem II at a resolution of 1.9Å. *Nature* 473, 55–60. doi: 10.1038/nature09913

Vass, I., and Styring, S. (1991). pH-dependent charge equilibria between tyrosine-D and the S states in photosystem II. Estimation of relative midpoint redox potentials. *Biochemistry* 30, 830–839. doi: 10.1021/bi00217a037

Vinyard, D. J., Ananyev, G. M., and Dismukes, G. C. (2013). Photosystem II: the reaction center of oxygenic photosynthesis. *Annu. Rev. Biochem.* 82, 577–606. doi: 10.1146/annurev-biochem-070511-100425

Vinyard, D. J., Khan, S., and Brudvig, G. W. (2015). Photosynthetic water oxidation: binding and activation of substrate water for O-O bond formation. *Faraday Discuss.* 185, 37–50. doi: 10.1039/c5fd00087d

Vrettos, J. S., Limburg, J., and Brudvig, G. W. (2001). Mechanism of photosynthetic water oxidation: combining biophysical studies of photosystem II with inorganic model chemistry. *Biochim. Biophys. Acta* 1503, 229–245. doi: 10.1016/S0005-2728(00)00214-0

Wang, J., Armstrong, W. H., and Batista, V. S. (2021). Do crystallographic XFEL data support binding of a watermolecule to the oxygen-evolving complex of photosystem II exposed to two flashes of light? *Proc. Natl. Acad. Sci. U. S. A.* 118:e2023982118. doi: 10.1073/pnas.2023982118

Wang, J., Askerka, M., Brudvig, G. W., and Batista, V. S. (2017). Crystallographic data support the carousel mechanism of water supply to the oxygen-evolving complex of photosystem II. *ACS Energy Lett.* 2, 2299–2306. doi: 10.1021/acsenergylett.7b00750

Wei, X., Su, X., Cao, P., Liu, X., Chang, W., Li, M., et al. (2016). Structure of spinach photosystem II–LHCII supercomplex at 3.2Å resolution. *Nature* 534, 69–74. doi: 10.1038/nature18020

Wieghardt, K. (1989). The active-sites in manganese-containing metalloproteins and inorganic model complexes. *Angew. Chem. Int. Ed.* 28, 1153–1172. doi: 10.1002/anie.198911531

Xiao, Y., Huang, G., You, X., Zhu, Q., Wang, W., Kuang, T., et al. (2021). Structural insights into cyanobacterial photosystem II intermediates associated with Psb28 and Tsl0063. *Nat. Plants* 7, 1132–1142. doi: 10.1038/s41477-021-00961-7

Yamaguchi, K., Shoji, M., Isobe, H., Yamanaka, S., Kawakami, T., Yamada, S., et al. (2018). Theory of chemical bonds in metalloenzymes XXI. Possible mechanisms of water oxidation in oxygen evolving complex of photosystem II. *Mol. Phys.* 116, 717–745. doi: 10.1080/00268976.2008.1428375

Yano, J., Kern, J., Irrgang, K. D., Latimer, M. J., Bergmann, U., Glatzel, P., et al. (2005). X-ray damage to the Mn_4Ca complex in single crystals of photosystem II: A case study for metalloprotein crystallography. *Proc. Natl. Acad. Sci. U. S. A.* 102, 12047–12052. doi: 10.1073/pnas.0505207102

Yano, J., and Yachandra, V. K. (2014). Mn_4Ca-cluster in photosynthesis: where and how water is oxidized to dioxygen. *Chem. Rev.* 114, 4175–4205. doi: 10.1021/cr4004874

Yao, R., Li, Y., Chen, Y., Xu, B., Chen, C., and Zhang, C. (2021). Rare-earth elements can structurally and energetically replace the calcium in a synthetic Mn_4CaO_4-cluster mimicking the oxygen-evolving center in photosynthesis. *J. Am. Chem. Soc.* 143, 17360–17365. doi: 10.1021/jacs.1c09085

Ye, S., Ding, C., Liu, M., Wang, A., Huang, Q., and Li, C. (2019). Water oxidation catalysts for artificial photosynthesis. *Adv. Mater.* 31:1902069. doi: 10.1002/adma.201902069

Yocum, C. F. (2008). The calcium and chloride requirements of the O_2 evolving complex. *Coord. Chem. Rev.* 252, 296–305. doi: 10.1016/j.ccr.2007.08.010

Young, I. D., Ibrahim, M., Chatterjee, R., Gul, S., Fuller, F. D., Koroidov, S., et al. (2016). Structure of photosystem II and substrate binding at room temperature. *Nature* 540, 453–457. doi: 10.1038/nature20161

Zhang, C. (2007). Low-barrier hydrogen bond plays key role in active photosystem II - a new model for photosynthetic water oxidation. *Biochim. Biophys. Acta* 1767, 493–499. doi: 10.1016/j.bbabio.2006.12.008

Zhang, C. (2015). The first artificial Mn_4Ca-cluster mimicking the oxygen-evolving center in photosystem II. *Sci. Chin. Life Sci.* 58, 816–817. doi: 10.1007/s11427-015-4889-1

Zhang, C., Chen, C., Dong, H., Shen, J. R., Dau, H., and Zhao, J. (2015). A synthetic Mn_4Ca-cluster mimicking the oxygen-evolving center of photosynthesis. *Science* 348, 690–693. doi: 10.1126/science.aaa6550

Zhang, C., and Kuang, T. (2018). A new milestone for photosynthesis. *Natl. Sci. Rev.* 5, 444–445. doi: 10.1093/nsr/nwx087

Zhang, C., Pan, J., Li, L., and Kuang, T. (1999). New structure model of oxygen-evolving center and mechanism for oxygen evolution in photosynthesis. *Chin. Sci. Bull.* 44, 2209–2215. doi: 10.1007/BF02885923

Zhang, J. Z., and Reisner, E. (2020). Advancing photosystem II photoelectrochemistry for semi-artificial photosynthesis. *Nat. Rev. Chem.* 4, 6–21. doi: 10.1038/s41570-019-0149-4

Zhang, B., and Sun, L. (2019a). Across the board: Licheng Sun on the mechanism of O-O bond formation in photosystem II. *ChemSusChem* 12, 3401–3404. doi: 10.1002/cssc.201901438

Zhang, B., and Sun, L. (2019b). Artificial photosynthesis: opportunities and challenges of molecular catalysts. *Chem. Soc. Rev.* 48, 2216–2264. doi: 10.1039/c8cs00897c

Zheng, M., and Dismukes, G. C. (1996). Orbital configuration of the valence electrons, ligand field symmetry, and manganese oxidation states of the photosynthetic water oxidizing complex: analysis of the S_2 state multiline EPR signals. *Inorg. Chem.* 35, 3307–3319. doi: 10.1021/ic9512340

Zouni, A., Witt, H. T., Kern, J., Fromme, P., Kraub, N., Saenger, W., et al. (2001). Crystal structure of photosystem II from *synechococcus elongatus* at 3.8 Å resolution. *Nature* 409, 739–743. doi: 10.1038/35055589

Conflict of Interest: The authors declare that the research was conducted in the absence of any commercial or financial relationships that could be construed as a potential conflict of interest.

Publisher's Note: All claims expressed in this article are solely those of the authors and do not necessarily represent those of their affiliated organizations, or those of the publisher, the editors and the reviewers. Any product that may be evaluated in this article, or claim that may be made by its manufacturer, is not guaranteed or endorsed by the publisher.